REPORT NO. DOT-TSC-FRA-71-8

PB 212 745

COMMUNICATIONS FOR HIGH SPEED GROUND TRANSPORTATION

GERALD CHIN
REUBEN EAVES
LOTHAR FRENKEL
RALPH KODIS

TRANSPORTATION SYSTEMS CENTER
55 BROADWAY
CAMBRIDGE, MA. 02142

NOVEMBER 15, 1971
TECHNICAL REPORT

Prepared for
DEPARTMENT OF TRANSPORTATION
FEDERAL RAILROAD ADMINISTRATION
WASHINGTON, D. C. 20591

The contents of this report reflect the views of the Transportation System Center which is responsible for the facts and the accuracy of the data presented herein. The contents do not necessarily reflect the official views or policy of the Department of Transportation. This report does not constitute a standard, specification or regulation.

TABLE OF CONTENTS

LIST OF ILLUSTRATIONS

LIST OF ILLUSTRATIONS (Cont)

LIST OF TABLES

SECTION 1. INTRODUCTION

The work at TSC on Communications for High Speed Ground Transportation has been divided into three categories, and analytical work has been done on each of these. No new problem areas have been uncovered, but some additional light has been shed on those that were known to exist. These problems may be divided into three categories: mechanical, electromagnetic, and communications. Although these will be dealt with separately in what follows, it should be emphasized that they are necessarily interrelated. Indeed, if there is any single major conclusion that emerges from our work on this task, it is that having disposed of most of the preliminary work, the OHSGT should seek to concentrate its efforts on a clearer definition of the mode of installation of the transmission line. Once this has been determined and tolerances set, the electromagnetic properties and communications characteristics of the line can be calculated readily, using well-established theories and computer techniques.

- MECHANICAL PROBLEMS

One of the environmental effects to which a long transmission line will be subjected is the expansion and contraction arising from temperature changes, day to night and winter to summer. A 90°F change in temperature will produce a 1.5 inch change in a 100 foot length of unrestrained aluminum transmission line. There are probably only two practical ways of dealing with this problem.

a) Fabricate a continuous line, installed in tension and restrained at very short intervals (or continuously) along a track or guideway.

b) Install the line with open expansion joints and low loss, low cost, well-matched bridging couplers.

Although a beginning has been made in the study of both of these problems, so much depends on engineering and cost considerations that little progress is possible without a better idea of the track or guideway configuration and the possible modes of installation. At the appropriate time these questions should be given the highest priority.

- ELECTROMAGNETIC PROBLEMS

The electromagnetic problems that need to be dealt with are set first of all by the required communication bandwidth. The basic command and control function, even with many cars on a single track, is relatively narrow band and could prob-

ably be handled by a straight forward open wire system without much trouble. When various communications functions are added on, however, the bandwidth may be increased to the point where a microwave carrier is required. If radio links are not feasible, some sort of open waveguide must be found. Of those available, a dielectric surface waveguide carrying the dominant hybrid mode is most attractive because of its physical simplicity, relatively low loss (for a waveguide), and relatively low dispersion. Of these the simple circular rod is probably optimum.

Since the characteristics of a uniform section of almost any useful waveguide can be computed with relative ease, the only significant problem associated with such a line derives from the extremely long lengths involved. A transmission line hundreds of miles long is necessarily non-uniform. Even if extreme care is exercised during fabrication and installation, irregularities will exist, some random, some periodic. These will result in non-uniform amplitude and phase characteristics as a function of frequency that strongly affect the choice of communications technique to be used with the line. At the State University of New Mexico such non-uniform characteristics have been constructed on a computer and have been exercised against some modulation techniques. The results are only indicative, however, and must remain so until something closer to the actual situation that is likely to exist can be specified.

Our studies at TSC indicate that the surface waveguide developed by the General Applied Science Laboratory has many of the desirable features one might specify in at least as good measure as any other that has been proposed or that comes to mind. We have also determined that planned bends on an open waveguide which follow curves of the track or guideway entail no serious radiation, loss, or reflection.

• COMMUNICATIONS PROBLEMS

The demands imposed on any communications systems in terms of cost, complexity and reliability are related directly to the communications bandwidth. This is especially true of a long transmission line where the non-uniformities that will inevitably be present produce transmission variations as a function of frequency that lead to ever increasing distortion and error. This problem is compounded by the inherently large losses associated with microwave transmission and the consequent need for large numbers of repeaters. Signal regeneration leads to further degredation unless some form of pulse code modulation is used, which means further increase in the bandwidth required. On the other hand, the

higher initial cost and complexity of a PCM system is offset by greater reliability and better signal-to-noise ratios (or fewer repeaters for the same S/N ratio).

• CONCLUSIONS AND RECOMMENDATIONS

Our study of the problem of high speed ground communications systems has made it clear that the mechanical, electromagnetic, and electronic problems associated with long microwave transmission lines are so closely interrelated that a subsystem study is needed to determine the cost per unit bandwidth of the various alternatives before any serious design work can begin. Such a study presupposes an early determination of a number of specifications for the overall high-speed ground system: i.e. rail or air cushion; degree of reliability; degree of redundancy; least acceptable and maximum desirable levels of service; environmental factors; etc. It could then proceed to transform the communications requirements into bandwidth, and the bandwidth requirements into transmission line specifications including manufacturing and installation tolerances. Only in this way could one hope to arrive at estimates of the cost of each increment in performance above the minimum needed for reliable train control. At this early stage the most that can be said is that if the mechanical and material requirements can be met at reasonable cost, the electromagnetic and electronic technologies exist to accomplish the necessary communications tasks.

SECTION 2.

MECHANICAL PROPERTIES OF LONG RIGID LINES

GENERAL CONSIDERATIONS

Since the propagation characteristics of an open waveguide will be adversely affected by snow or water, it is undesirable to support the guide close to the track facing upward. This leaves the possibilities of suspending the ribbon overhead in the manner of a catenary or of supporting it rigidly in a vertical plane. (The latter method may, perhaps, be considered desirable for installation into the channel-type track for TACV's.)

The thermal expansion of rails can cause buckling. This tendency is aggravated in the case of welded rails. Since the coefficients of thermal expansion for Al and Cu are larger than that for steel it is to be expected that the problems will be more severe for the waveguide. In the case of a freely suspended ribbon the sag between supports could provide for expansion. For this configuration it is of interest to examine the restrictions of the radius of curvature imposed by the elastic limits of the materials. In the case of a ribbon constrained to the vertical part of the track it is of interest to establish virtual strains in relation to the elastic limits and to calculate critical loads for a given number of supports.

TABLE 1. THERMAL AND ELASTIC PROPERTIES OF SOME MATERIALS.

	Al	Cu	Fe
Coefficient of expansion per deg. C	24×10^{-6}	15×10^{-6}	12×10^{-6}
Modulus of elasticity dynes/cm^2	6×10^{11}	12×10^{11}	20×10^{11}
Modulus of elasticity lbs/sq. inch	8.4×10^{6}	17×10^{6}	29×10^{6}
Tensile elastic limit dynes/cm^2	1×10^{9}	1.5×10^{9}	3.2×10^{9}
Tensile elastic limit lbs/sq. inch	1.4×10^{4}	2.0×10^{4}	4.5×10^{4}

The relevant properties of some materials are listed above. Using Table 1 we shall calculate nominal values of the thermal expansion, ΔL, for a 10 m (30 Ft.) section and the force, F, required to restrain such a section to maintain its length. We shall assume that the total cross section of the ribbon is about 6 cm^2 (1 sq. inch). The temperature differential will be assumed to be 50° C (90° F). For these conditions we find the values listed in Table 2.

TABLE 2. THERMAL AND ELASTIC DEFORMATION OF RIGID TRANSMISSION LINE.

		Al	Cu	Fe
ΔL	cm	1.2	.75	.6
	in	.5	.3	.24
F	dynes	42×10^8	54×10^8	72×10^8
	lbs	$10. \times 10^3$	13×10^3	17×10^3
$\Delta L'$	cm	1.6	1.3	1.6
	in	.6	.5	.6

In Table 2 $\Delta L'$ is the virtual expansion when the material is stressed to the elastic limit. A comparison of ΔL and $\Delta L'$ for the various materials shows that aluminum would be stressed close to its tensile elastic limit if constrained to maintain its length, and the situation for copper is not much better. It also appears that the forces developed along the line amount to about 5 tons; this is an important factor to remember when designing supports. For example, if the line is straight, the forces between sections cancel so that provisions for taking up the stress are required only where the line terminates. If, however, one section buckles the full stress may be placed on one or two supports. This will be discussed later.

MECHANICAL CONSIDERATIONS

OVERHEAD SUSPENSION. In this section we shall calculate some of the data necessary for a semiquantitative discussion of the problem involved in overhead suspension of the line. If the line is again assumed to be supported at 10 m intervals, it will bend under its weight between supports. Except for the effects of the bending moments, the line would then form a catenary. We are interested in three quantities: (a) the amount of sag assuming that no tension or compression is applied at the ends of each section; (b) the additional sag due to thermal expansion;

and (c) extreme fibre stress at the points of maximum flexure. We shall assume that the guide forms an H-beam of horizontal dimensions of 10 x .3 cm (4" by .14") and vertical dimensions for each of the legs of 2.5 x .3 cm (1" x .14"). We shall assume that the weight of the line for aluminum is 27 gr/cm (2.5 oz per inch). With these values we get the approximate numbers in Table 3.

TABLE 3. THERMAL AND ELASTIC DEFORMATION OF SUSPENDED TRANSMISSION LINE.

		Al	Cu	Fe
sag	(cm)	20	40	20
	(in)	8	16	8
Δ sag	(cm)	22	17	15
	(in)	9	7	6
Max. fibre stress	($dynes/cm^2$)	1×10^9	2.5×10^9	2×10^9
	(lb/sq inch)	1.4×10^4	3.5×10^4	2.8×10^4
Weight	gr/cm	27	62	55
	oz/inch	2.5	5.5	5

In Table 3 Δ sag is the additional sag which would result from thermal expansion.

It should be noted that the maximum fibre stress (Table 3) exceeds the elastic limits for aluminum and copper and does not provide for much of a margin even in the case of iron. A rough estimate of the additional forces resulting from the updraft to be expected from the train shows that the additional loading may be as large as 50-60 grams per cm of line (5 oz. per inch). A comparison with Table 3 shows that this represents a threefold increase of the loading in the case of aluminum. On the other hand, the sag for the 10 meter supports is just about adequate to accommodate thermal expansion. Thus, if the manner of support is changed to reduce fibre stress, one would expect problems with longitudinal forces tending to buckle or twist the line. Furthermore, updraft and downdraft may pose severe problems for any plastic covering over the line

RIGID INSTALLATION AND CRITICAL LOADS. If the line is supported in a vertical plane and constrained to hold its shape, a sufficient number of support points must be provided so that

the thermal stress does not exceed the critical load for each section. Table 4 gives critical loads for 10 meter supports and the number of supports required for the loading F of Table 2.

TABLE 4. STRESS LIMITS FOR RIGID LINE USING 10 M SUPPORTS AND ACTUAL NUMBERS OF SUPPORTS REQUIRED.

		Al	Cu	Fe
Critical load for 10 m supports	(dynes)	3×10^7	7×10^7	12×10^7
	(lbs)	$.8 \times 10^2$	1.6×10^2	2.8×10^2
Max. distance between supports for load = F	(meters)	.8	1.	1.2
	(feet)	2.4	3.	4

The number of points of attachment required for a rigid installation of the line is found to be comparable to the number of ties required for rails. There is, however, no obvious cheap analogue to ties and gravel ballast that could be used in the installation of the line in a vertical support structure. The shape of the extruded piece could be arranged so that it could be seated against suitably shaped supports and clamped at the edges. The clamping, however, would seem to require prefabricated machined parts of some complexity.

CONCLUSIONS

For the cross sectional shape considered here the requirements for withstanding thermal stresses are rather severe. These calculations lead to the conclusion that the installation of a continuous line will require a detailed engineering effort. The rigid installation appears to be more tractable but will be quite expensive. Finally, the results suggest that a configuration using matched couplings in combination with expansion joints should receive close attention. The task here is to design a broad band transition to bridge the expansion joints. Such transitions must be reasonably inexpensive and above all must be free from reflections over the bandwidth employed in this communications system.

SECTION 3.

ELECTROMAGNETIC PROPERTIES OF SURFACE WAVE COUPLERS

Consideration of the mechanical problems associated with thermal effects on a continuous transmission line has shown that a rigid line constrained to the guideway is feasible and offers the advantages of low loss and freedom from multiple reflections. A less costly alternative, however, may be a segmented line with expansion joints, bridged by coupling transitions similar to the parallel coupled lines proposed by GASL for their repeater stations. In this report the electromagnetic properties of such an expansion joint are examined in order to estimate:

a. The coupling losses due to thermal expansion and wide band operation.

b. The reflection coefficient introduced at each point.

The model we have in mind for the purpose of this discussion is the dielectric rod line which has been treated in detail elsewhere.* However, the formulation applies equally well to any configuration of conductors and dielectrics which is transversely inhomogeneous, but axially uniform and on which a single transverse electromagnetic mode is progagating. In each dielectric region (such as the interior of a dielectric rod) the axially propagating wave is completely characterized by an equivalent transmission line whose shunt admittance and series impedance per unit length are given by:

$$Y = \frac{k^2-\omega^2\varepsilon\mu}{Z} \text{ mho/meter} \qquad (1)$$

$$Z = \frac{k^2-\omega^2\varepsilon\mu}{Y} \text{ ohm/meter} \qquad (2)$$

The particular values of Y and Z are determined by the geometry and the mode being considered. For predominantly H-mode coupling, $Z = j\omega\mu$; for predominantly E-mode coupling $Y = j\omega\varepsilon$, where ε and μ are the dielectric and magnetic constants of the

*For example:
Gen. Appl. Sci. Labs, Inc., Tech. Rept. 729, Final Report on Contract DOT-FR-9-0016 of 1 August 1969.
Collin, R. E. "Field Theory of Guided Waves," McGraw Hill, New York 1960.

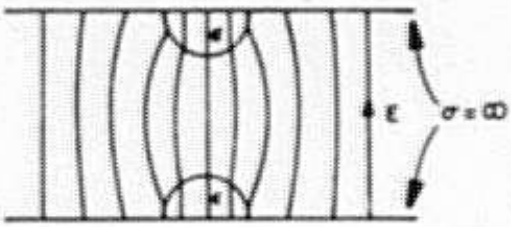

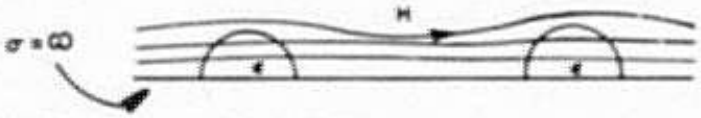

Figure 1a. H-Mode Coupling

Figure 1b. E-Mode Coupling

medium. For a hybrid mode, as well as for either of its constituents, the propagation constant γ is defined by

$$\gamma^2 = k^2 - \omega^2 \varepsilon \mu = YZ \qquad (3)$$

In all of these relations, k is the transverse eigenvalue determined by the particular geometry and mode. As ε varies from point to point in the transverse plane, k changes its value in such a way as to keep γ constant.

As an aid in applying transmission line techniques, consider the GASL dielectric image line, two parallel sections of which may be coupled in either of the simple configurations shown schematically in Figure 1. Figure 1a. is an E-field (H-mode) coupler as proposed by GASL for train-to-wayside. The H-field (E-mode) coupler of Figure 1b. is perhaps better suited for either a bridging or repeater application. In any case, we shall use this mode as an example in what follows.

For a single E-mode propagating as $e^{\gamma z}$ on a uniform transmission line a pair of complex functions, V and I, may be defined which satisfy the first order linear differential equations:

$$\frac{dI(z)}{dz} = -YV(z) \quad ; \; Y = j\omega c \tag{4}$$

$$\frac{dV(z)}{dz} = -ZI(z) \quad ; \; Z = \gamma^2/Y \tag{5}$$

If an identical pair of such lines is coupled through an admittance Y_{12}, an equivalent circuit representation of an elementary section of the coupled transmission lines is shown in Figure 2. The coupling admittance makes it necessary to modify eq.4 for line #1 as follows:

$$\frac{dI_1}{dz} = -YV_1 + Y_{12}(V_2 - V_1) \tag{6}$$

A similar set of equations can be written for line #2 by an interchange of subscripts. The elimination of I_1 and I_2 leads to a pair of coupled second-order equations for V_1 and V_2. They are

$$\frac{d^2V_1}{dz^2} - (Y + Y_{12})\, ZV_1 = Y_{12}ZV_2 \tag{7}$$

$$\frac{d^2V_2}{dz^2} - (Y + Y_{12})\, ZV_2 = Y_{12}ZV_1 \tag{8}$$

Assuming that the solutions have the form $V_1 = A \exp(\gamma z)$; $V_2 = B \exp(\gamma z)$, one can show by direct substitution that there are two modes of propagation

1) $\gamma_a^2 = YZ \; ; \; B = A$

The phase velocity v_p for this mode is the same as for the unperturbed line (See equation 3). Since V_1 and V_2 are in phase opposition it may be called the antisymmetric mode with $\gamma a = j\beta_q = -j\omega/v_p$, where v_p is the phase velocity on the unperturbed line.

2) $\gamma_s^2 = YZ\,(1 + 2Y_{12}/Y) \; ; \; B = A$

For the E-mode under consideration Y_{12} is inductive, while Y is capacitative. For H-mode (E-field) coupling, the reverse would be true. In either case, the phase velocity is increased over that of the unperturbed line. This propagation mode is called symmetric with $\gamma_s = -j\beta_g\,(1 + 2Y_{12}/Y)$.

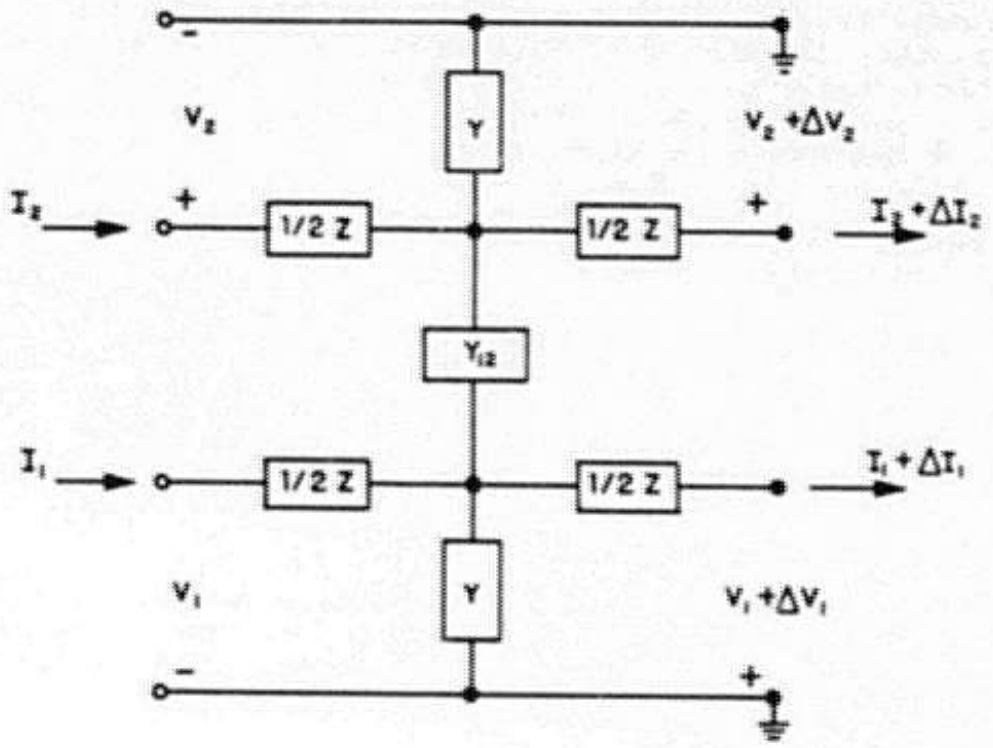

Figure 2. Equivalent Circuit for an Element of Coupled Transmission Lines.

The general solution of (7) and (8) is a linear combination of symmetric and antisymmetric modes. Following the GASL procedure, we assume that they propagate in the +z direction with equal amplitudes and write:

$$V_1 = A(e^{\gamma_s z} + e^{\gamma_a z}) \tag{9}$$

$$V_2 = A(e^{\gamma_s z} - e^{\gamma_a z}) \tag{10}$$

Substitution leads at once to:

$$V_1 = 2A \cos \left[(Y_{12}/Y)\beta_g z\right] \; e^{-j\left[1+(Y_{12}/Y)\right]\beta_g z}$$

$$V_2 = -2jA \sin \left[(Y_{12}/Y)\beta_g z\right] e^{-j\left[1+(Y_{12}/Y)\right]\beta_g z}$$

These results are similar to those reported by GASL. Their added significance is that they have been derived in a general way so that they apply to any coupling mode for any single transverse mode of operation. Note that if a positive, real coupling constant is defined according to:

$$K = -Y_{12}/Y \tag{11}$$

then for $K = 0$, V_2 vanishes and V_1 reduces to the usual function for a single line.

In the case of a dielectric rod operating in the HE_{11} mode the required conditions are closely approximated at frequencies low enough so that $v_p \approx c$, the speed of light. In this situation, which is characteristic of the GASL line, $k^2 << \omega^2\varepsilon\mu$, E_z and $H_z \approx 0$, and the field configuration is predominantly TEM.

COUPLING LOSSES

The coupling losses due to thermal expansion and wide-band operation depend upon the way in which the power density on the line varies with distance and wavelength. The power distribution, P_1, on the primary transmission line is:

$$P_1 = \frac{1}{2} \mathrm{Re}(V_1 I_1^*).$$

Using (9) and (5), we find that

$$P_1(z) = \frac{2A^2}{\omega\mu} (1-K)\beta_g \cos^2 (K\beta_g z). \tag{12}$$

Thus, the maximum power that can be transferred from the primary line to the bridging section is:

$$P_o = \frac{2A^2}{\omega\mu} (1-K)\beta_g. \tag{13}$$

Clearly, the coupling process itself introduces an unavoidable loss given by the factor (1-K).

The maximum available power, given by (12) is transferred whenever $K\beta_g z = (2n+1)\,\pi/2$ so that the bridging distance for maximum power transfer is:

$$z_m = \tfrac{1}{4}\lambda_g (2n+1)/K, \tag{14}$$

while n is any positive integer. It should be noted that while more power is transferred for smaller K, the coupling length z_m must be increased as K is decreased.

EXPANSION LOSS

When thermal expansion disturbs the line length adjustment given by (14) so that $z = z_m + \Delta z$, power is transferred from line 2 back to line 1. The amount of power which is dissipated and lost in the matched termination of line 1 for small Δz is:

$$\Delta P_1(z)_{\beta_g=\text{const}} = -\frac{4A^2}{\omega\mu} K(1-K)\beta_g^2 \cos(K\beta_g z) \sin(K\beta_g z)(\Delta z). \tag{15}$$

For $K\beta_g \Delta z \ll 1$, eqs. (13), (14) and (15) lead to the approximate results:

$$\left[\frac{\Delta P_1(z)}{P_o(z_m)}\right]_{\beta_g=\text{const}} \approx 2(K\beta_g)^2(\Delta z)^2 = 2\left[(2n+1)\pi/2\right]^2\left(\frac{\Delta z}{z_m}\right)^2. \tag{16}$$

The last part of this equation follows from (14). Equation (16) represents the fraction of the carrier power which is lost at the end of one section of transmission line. It is again seen to be advantageous to keep K, the coupling ratio at the bridging transitions, as small as possible.

BANDSPREAD LOSS

Since the coupling of power from the primary line to the bridging section and back is a resonant phenomenon, a differential power loss will exist over the frequency band being transmitted. To calculate this differential let us assume that the bridging length is optimized at $z = z_m$. Then

$$\Delta P_1(\omega)_{z=z_m} = -\frac{4A^2}{\mu v_p^2} K(1-K) z_m \cos(K z_m \omega/v_p) \sin(K z_m \omega/v_p)\,(\Delta\omega) \tag{17}$$

Set $\omega = \omega_o + \Delta\omega$. Then for $\Delta\omega/\omega_o << 1$

$$\left[\frac{\Delta P_1(\omega)}{P_o(\omega_o)}\right]_{z=z_m} \approx 2\left[(2n+1)\pi/2\right]^2\left(\frac{\Delta\omega}{\omega_o}\right)^2 . \qquad (18)$$

This result indicates that the integer n should be chosed to be as small as possible, which means that other things being equal, the coupling distance z_m should be as small as possible in order to reduce the differential loss over the band. The design of the bridging transition is thus seen to involve the mutual adjustment of a number of parameters. Some alternatives will be examined in the following section of this report.

EXAMPLES

The data to be used for some typical calculations are:

(a) The coefficient of expansion for copper,

$$\epsilon = 1.5 \times 10^{-5}/\text{deg C};$$

(b) the temperature increment,

$$\Delta T = 50 \text{ deg C};$$

(c) the primary line section length to the nearest integral number of half-wavelengths,

$$L = p\lambda_o/2.$$

With these data, the expansion loss takes the form:

$$\Delta P_1(z)/P_o(z_m) = 2\pi^2\left[\epsilon(\Delta T)(pK)\right]^2. \qquad (19)$$

For both (18) and (19) the coupling loss per line section in dB is:

$$10 \log_{10} \frac{P-\Delta P_1}{P_o} \approx -4.34 \frac{\Delta P_1}{P_0} \text{ dB} \qquad (20)$$

These formulas have been used in the preparation of Figures 3 and 4 which show the expansion and dispersion loses in dB per km to be expected for various line lengths, bandwidths, and coupling ratios. With these charts, expansion joints could be designed

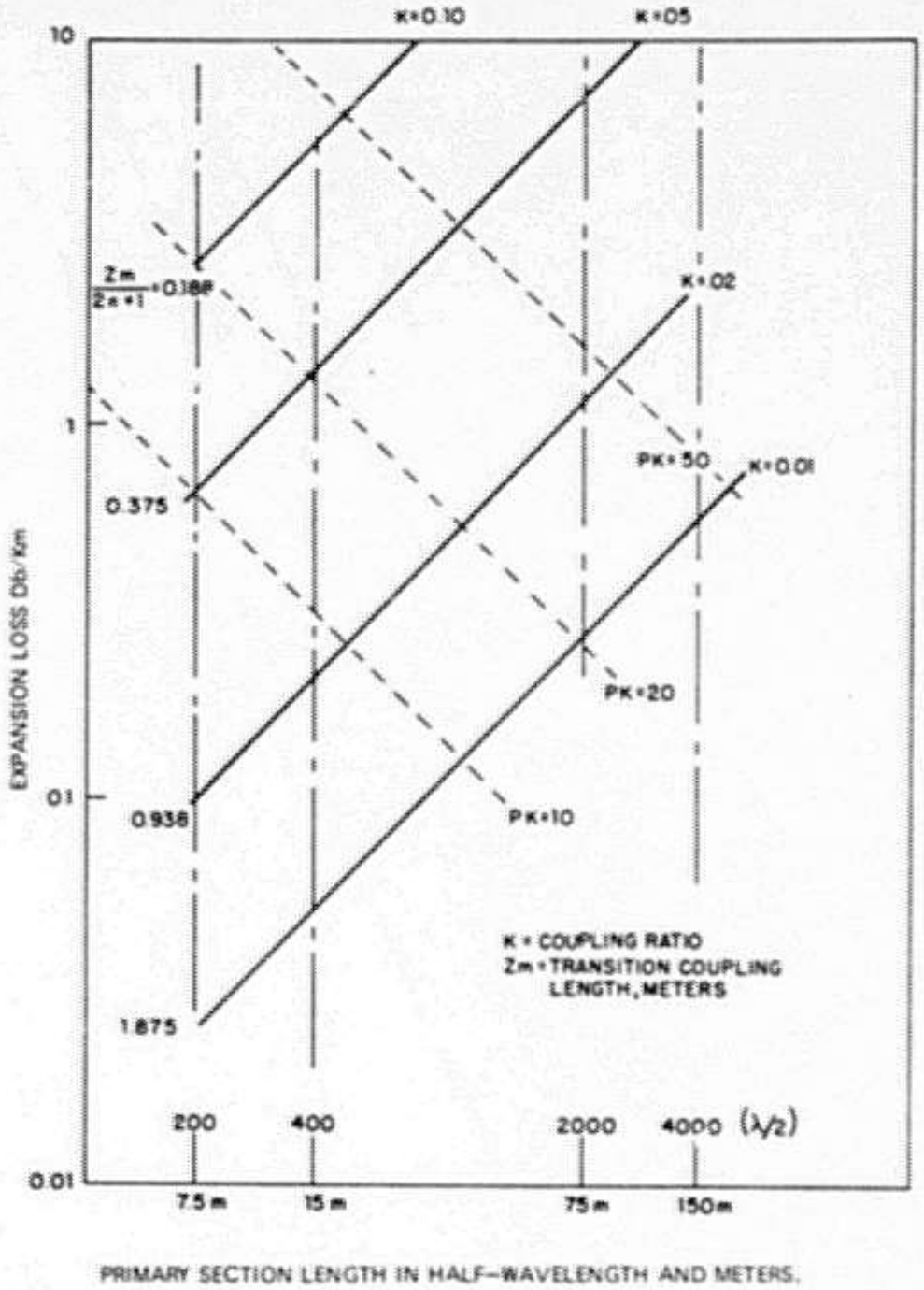

Figure 3. Expansion Loss Versus Primary Section Length

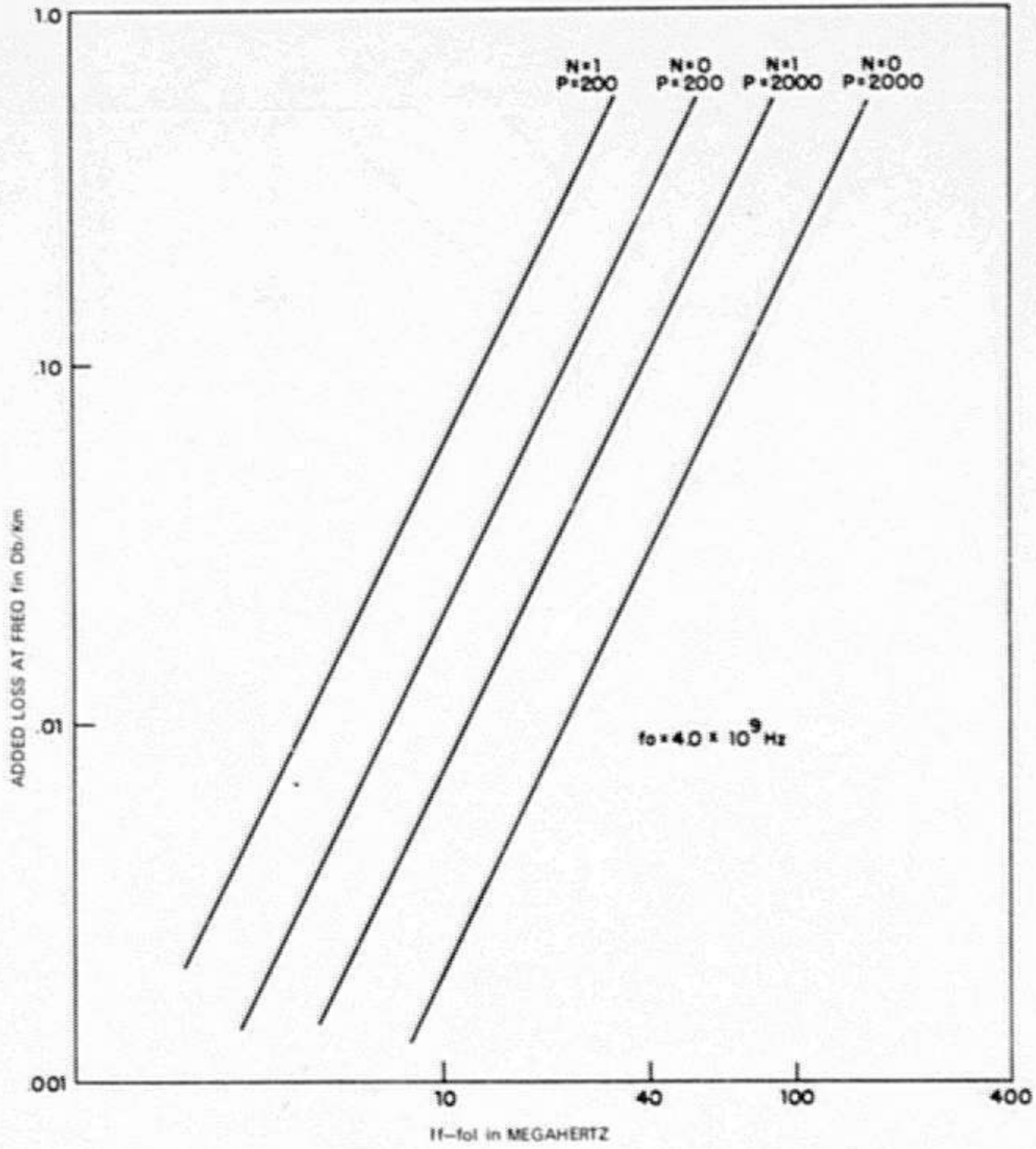

Figure 4. Bandspread Loss

to fit the various performance and engineering requirements of the transmission line.

REFLECTION LOSSES

At each bridging transition, the characteristic impedance of the primary line changes more or less abruptly, leading to reflections which lead to further reductions in the power transmitted down the line. If the voltage reflection coefficient is R, the power transmitted per unit incident power is

$$(P_t)_1 = 1-|R|^2. \tag{21}$$

The reflection coefficient, in turn, is

$$R = \frac{Y_o-Y_1}{Y_o+Y_1} \tag{22}$$

where Y_1 and Y_o are the characteristic admittances of the coupled and the unperturbed lines, respectively. For the case under consideration

$$Y_o = (Y/Z)^{\frac{1}{2}} = (k^2-\beta_g^2)^{\frac{1}{2}}/Z \approx \beta_g/\omega\mu \tag{23}$$

$$Y_1 = I_1/V_1 = Y_o\left[(1-K) - jK\tan(K\beta_g z)\right]. \tag{24}$$

Note that $Y_o \approx G_o$, a pure conductance, while Y_1 is complex and depends on position. For zero coupling, $K = 0$ and $Y_1 = Y_o$ as expected, while for $K = 1$ the characteristic admittance is purely imaginary, which means that no propagating wave exists and the incident energy is totally reflected.

At the entrance to the bridging section, where the power in the primary line is maximum, $z = 0$ and

$$Y_1 = G_1 = G_o(1-K)$$

Thus, the reflection coefficient is real and equal to:

$$R = \frac{K}{2-K} \tag{25}$$

Taking as an example a line with 100 expansion joints, we find that the power transmitted per unit incident power at mid-band and optimum z_m for a lossless line is

$$P_t = (1-R^2)^{100} .$$

In total dB, for $R^2 \ll 1$,

$$10 \log_{10} P_t = 4.34 \times 10^3 R^2 . \qquad (26)$$

Typical results are tabulated below:

		P_t/P_o	P_r/P_o
K	R	100 sections	single section
0.01	5.02×10^{-3}	-0.1 dB	-46 dB
0.02	1.01×10^{-2}	-0.4 dB	-40 dB
0.05	2.56×10^{-2}	-2.8 dB	-32 dB
0.10	5.26×10^{-2}	-12.0 dB	-26 dB

These reflection losses are frequency independent. At frequencies separated by the approximate interval

$$\Delta f \approx \frac{1}{p} f_o , \qquad (27)$$

where p is the number of half-wavelengths on the primary section, the transfer function will also exhibit the characteristic comb filter effect.

SECTION 4.

ELECTROMAGNETIC PROPERTIES OF BENDS IN SURFACE WAVE LINES

THE GEOMETRY OF BENDS

The degree of bending in a waveguide can be measured either in terms of the radius of curvature, R, or in terms of the maximum deviation, δ, from a straigh line over a distance, d. Bends required by planned curves in the track are conveniently specified by the radius of curvature; those otherwise produced are more easily described by the deviation per unit distance. These different kinds of bends may be compared by means of the following relation (Figure 5):

$$R/d = \frac{1}{2} (\delta/d) + \frac{1}{8} (d/\delta).$$

The maximum allowable track curvature for a high-speed vehicle has a radius of 2-miles (3.2-km), which corresponds to a deviation of 3.9-millimeters over a distance of 10-meters. This is much smaller than the deviations that could result from thermal and other local effects which will probably be the principal sources of deviation loss. This is shown in Figure 6, where the radius of curvature is plotted against a given sag for various support separations.

RADIATION FROM BENDS

Radiation loss from curved open waveguides can occur in either of two ways: by continuous radiation over the length of the curve or by radiation at points where there is a discontinuous change in the radius of curvature of the guide. Loss of the first kind occurs over curves such as FG in Figure 7; loss of the second kind takes place in the neighborhood of points such as F, G, and H. These loss mechanisms are discussed in detail below.

RADIATION ALONG A BEND WITH CONSTANT RADIUS OF CURVATURE. If an electromagnetic wave were to maintain a uniform phase front and avoid loss while negotiating a bend in an open waveguide, the outer portion of the wave would have to speed up. Beyond a certain distance from the guide, however, the required velocity exceeds the velocity of light, so that phase fronts tend in fact to lag behind, leading to propagation away from the bend and loss of energy. The longitudinal distance over which the loss occurs determines the collimated beamwidth.

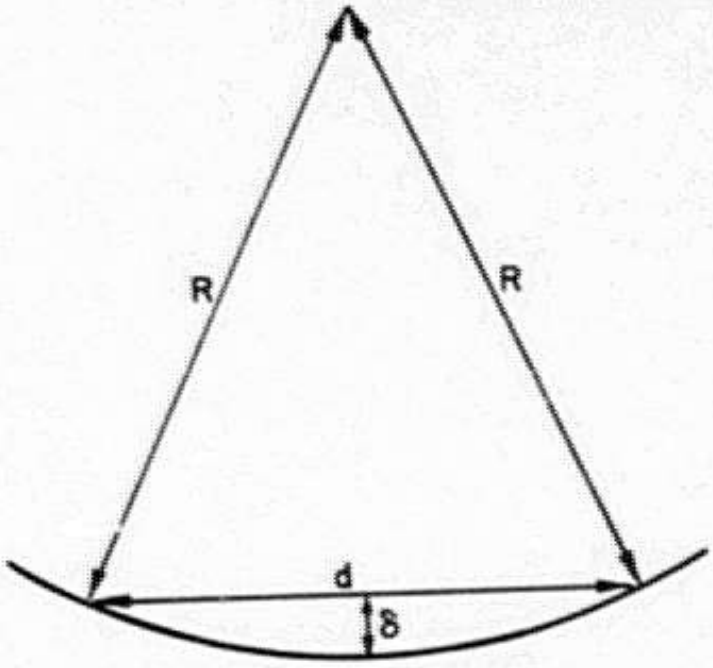

Figure 5. Geometry of a Waveguide Bend

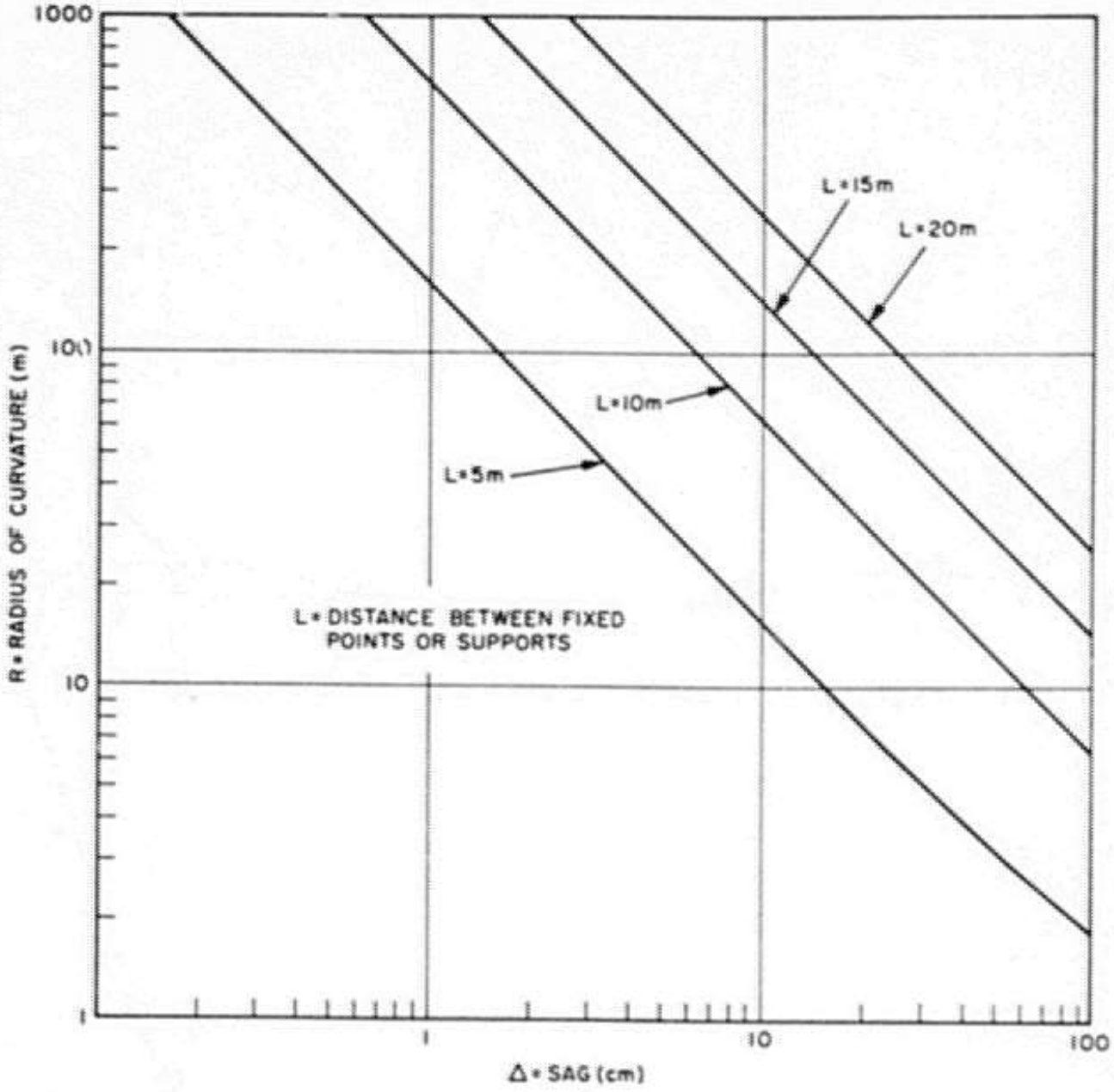

Figure 6. Curvature Produced by Sag or Other Deviations

For a dielectric rod in free space operating in the HE_{11} mode with $v_p/c \approx 1$, the field configuration is nearly TEM, and a bend of a given radius results in approximately the same loss regardless of the plane of the bend. The GASL line consists of one-half of such a dielectric rod mounted on a conducting shield. Because of the shield virtually all the energy on the line is confined to the half space ABD of Figure 8. Therefore, bends with A as a center occasion little loss since no energy is propagating on the convex side of the bend. Only those bends with radii of curvature in the half-space BCD need to be considered.

If one assumes that half a dielectric rod on an infinite, perfectly conducting plane surface is a good approximation to the GASL line of Figure 8, it is possible to compute the attenuation for bends of various curvature. The results are shown on Figure 9 for two centers of curvature at two different frequencies near the band limits. Loss of power is related to attenuation through the formula

$$dP/dz = - \alpha P.$$

On the assumption that all the lost power is radiated outward in one polarization and at one frequency into a 20° sector, the electric field intensity at 100-feet has been computed and is shown in Figure 10. In this worst case the FCC limit of 500 μV/m at 100 feet is exceeded only for bends of 40-meter radius or less.

Radiation at a Discontinuity in Radius of Curvature

A discontinuity in the radius of curvature of an open waveguide leads to radiation whose intensity may be estimated from a two-dimensional impedance plane model that has been discussed in the literature. Figure 11 shows a typical radiation pattern calculated for a discontinuity in the radius of curvature of such a plane. Similar patterns have been measured for bent dielectric rods. It turns out that although the intensity of the radiation decreased inversely with the square of the radius of curvature, its pattern depends only on c/v_p and becomes highly directive for $c/v_p \approx 1$.

The power loss that results from a discontinuous change in radius of curvature from zero to a large value of R is approximately

$$P_{sc} = \frac{1}{32\pi^2} (\lambda/R)^2 \left[(c/v_p)^2 - 1\right]^{-3}.$$

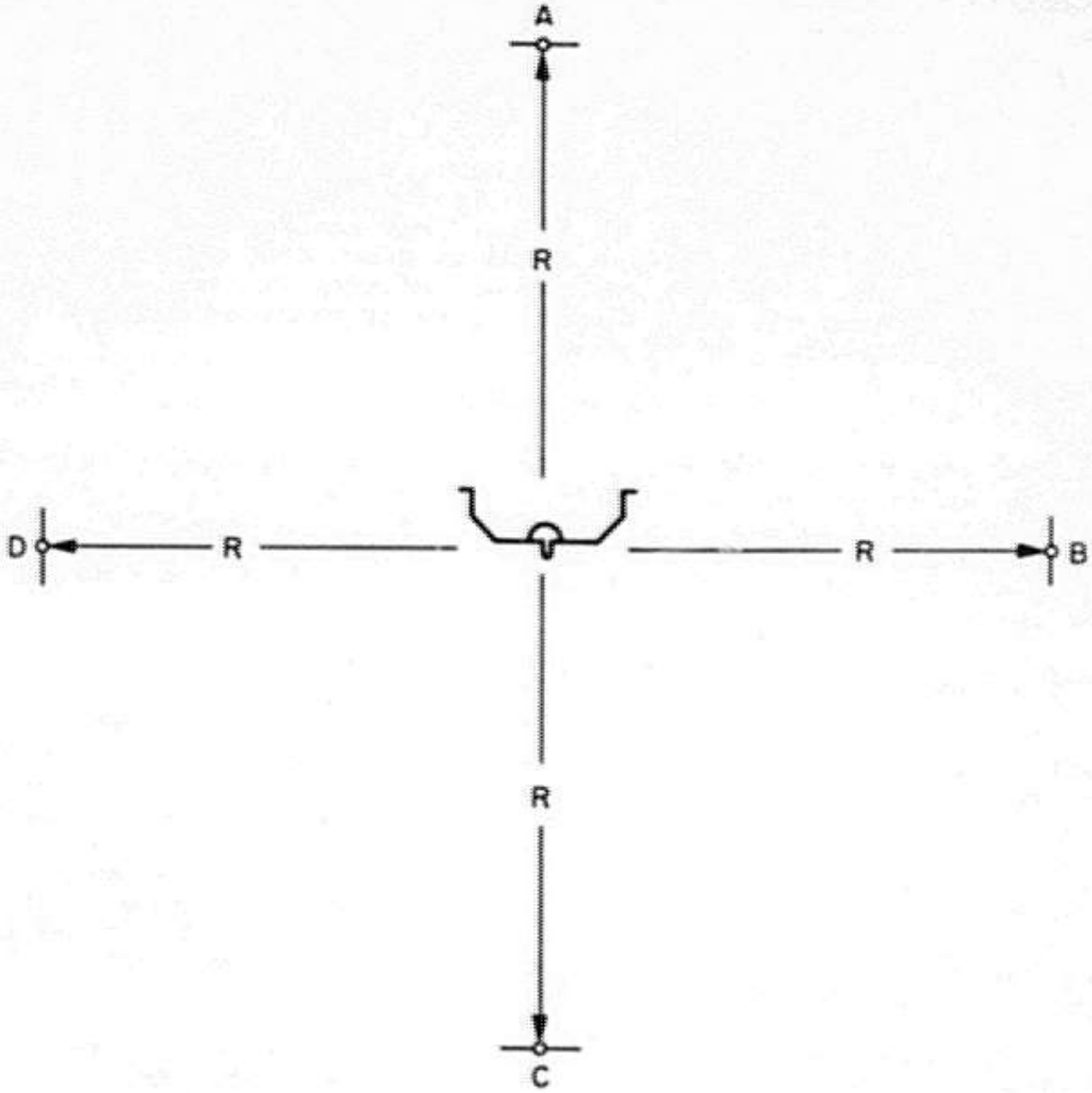

Figure 8. Possible Centers of Curvature

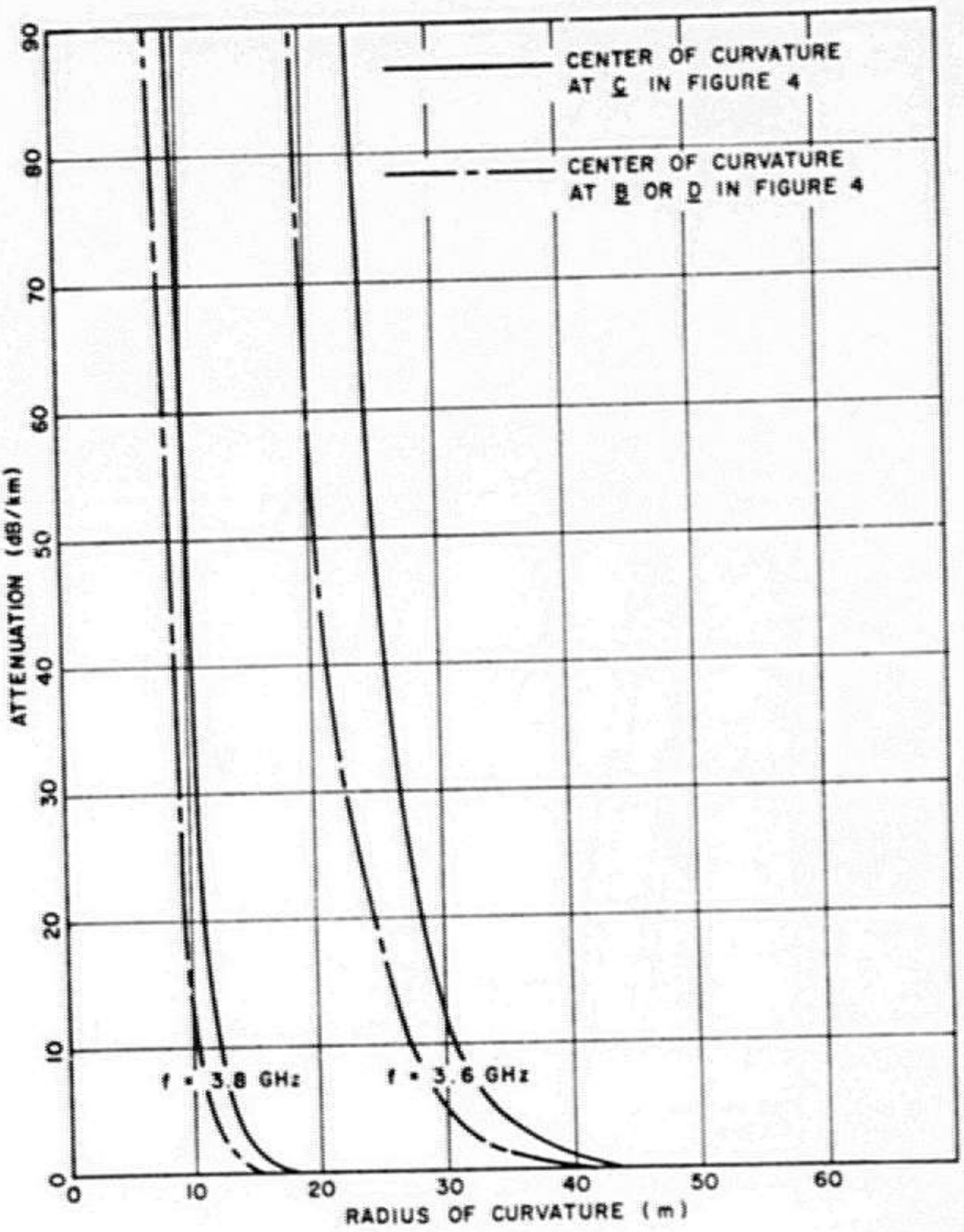

Figure 9. Attenuation Resulting from a Bend of Constant Radius of Curvature

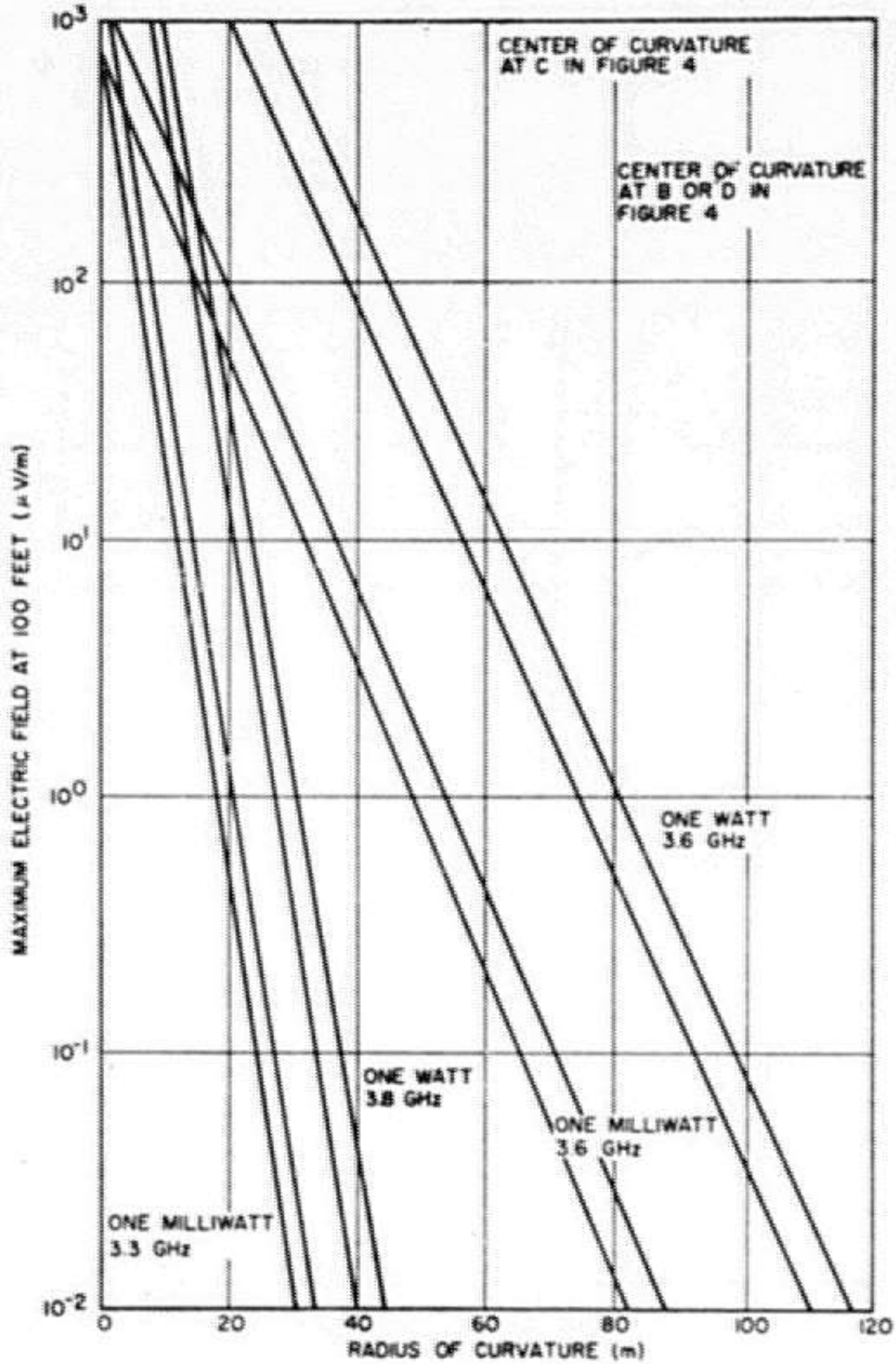

Figure 10. Electric Field at 100 Feet Resulting from a Bend of Constant Radius of Curvature

For the sinuous line of Figure 6., the change of curvature at the points of inflection is 2R. With 1/d inflection points per meter, the loss in dB/km may be computed from the above formula. Results are plotted in Figure 12. If it is further assumed that the energy lost is radiated into a cone whose half-angle corresponds to that calculated for the two-dimensional impedance plane (4^o - 6^o from 3.6 to 3.8 GHz), estimates can be made of the expected maximum electric field strength 30-meters from the line. The results are shown in Figure 13.

REFLECTION AT A CHANGE IN CURVATURE

A discontinuous change in curvature not only leads to loss but also excites a reflected wave on the line. The reflection coefficient can be estimated on the basis of the two dimensional model already used. At these frequencies it turns out to be

$$|\Gamma| \approx 10^{-3}/R$$

Reflections of this magnitude are negligible for all reasonable curvature fluctuations and are not considered further.

CONCLUSIONS

a. Radiation due to uniform bends is negligible (i.e. within FCC limits) if the radius of curvature exceeds 50 meters.

b. Discontinuous changes in the radius of curvature due to sag, thermal effects, etc. could easily produce radiation lobes that would exceed FCC limits and make the line susceptible to interference.

c. Reflection and mode conversion are negligible at bends of the kind likely to occur in a wayside transmission line.

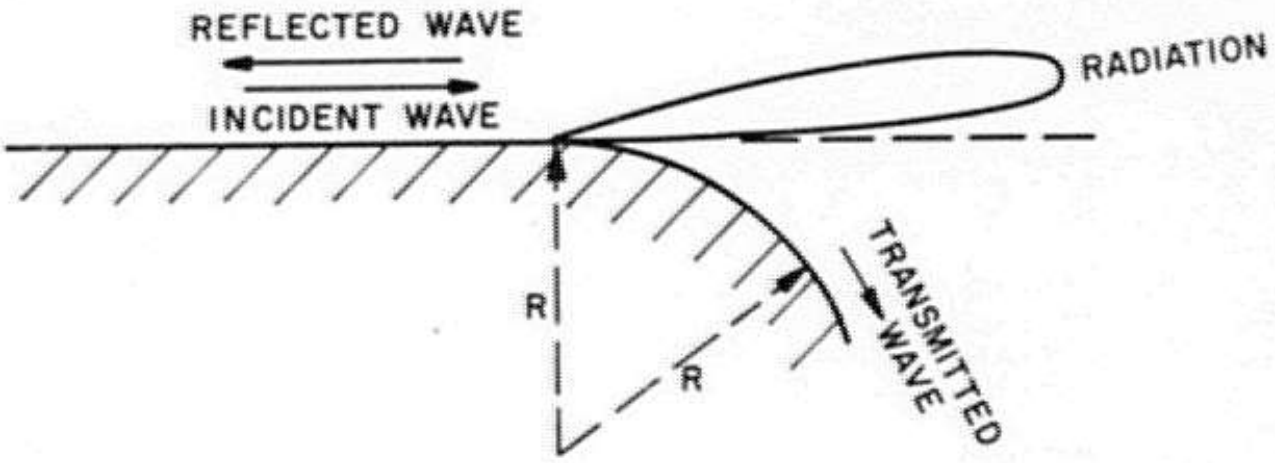

Figure 11. Radiation Pattern Produced by a Discontinuity in Radius of Curvature

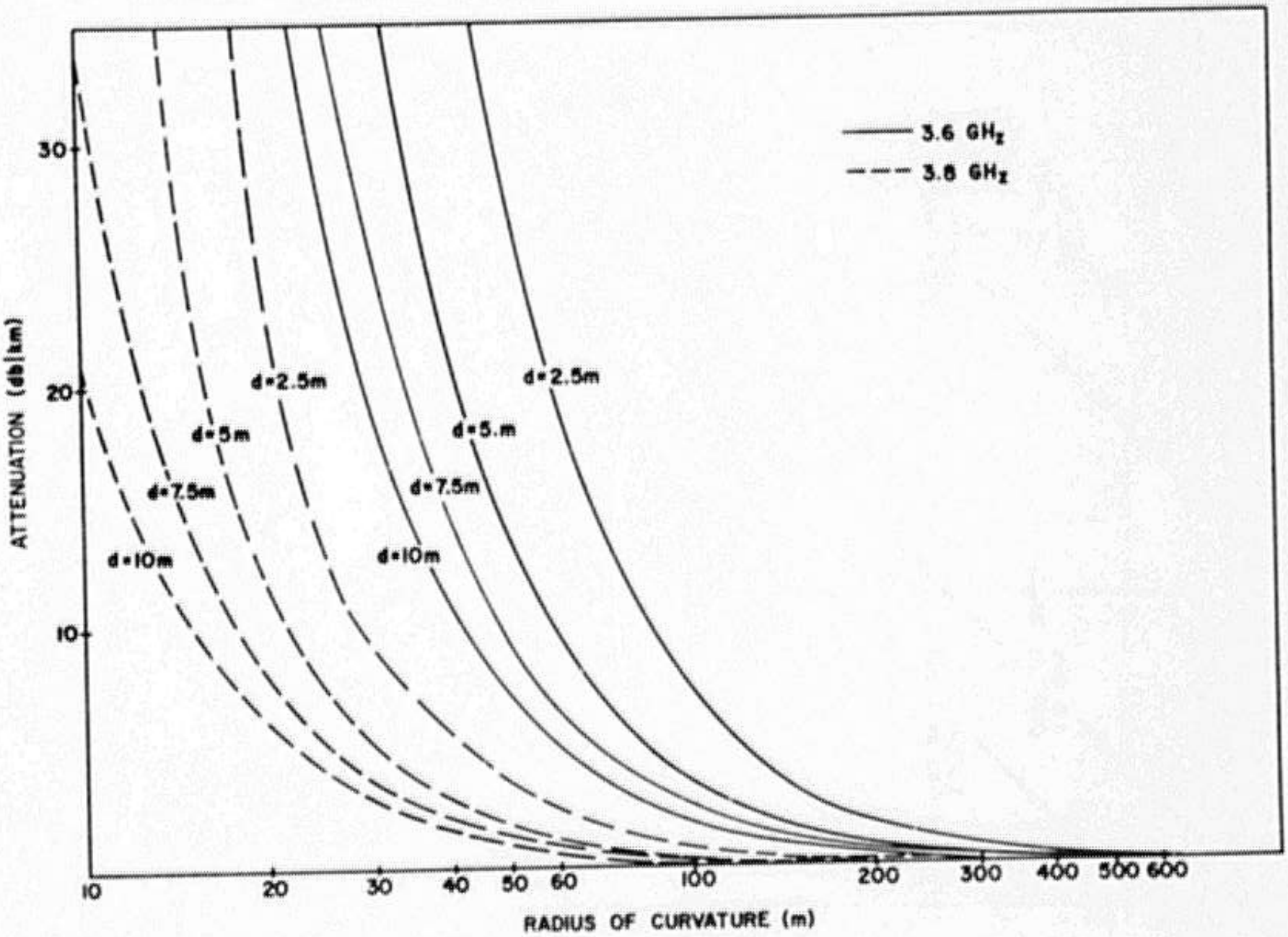

Figure 12. Attenuation of a Sinuous Line

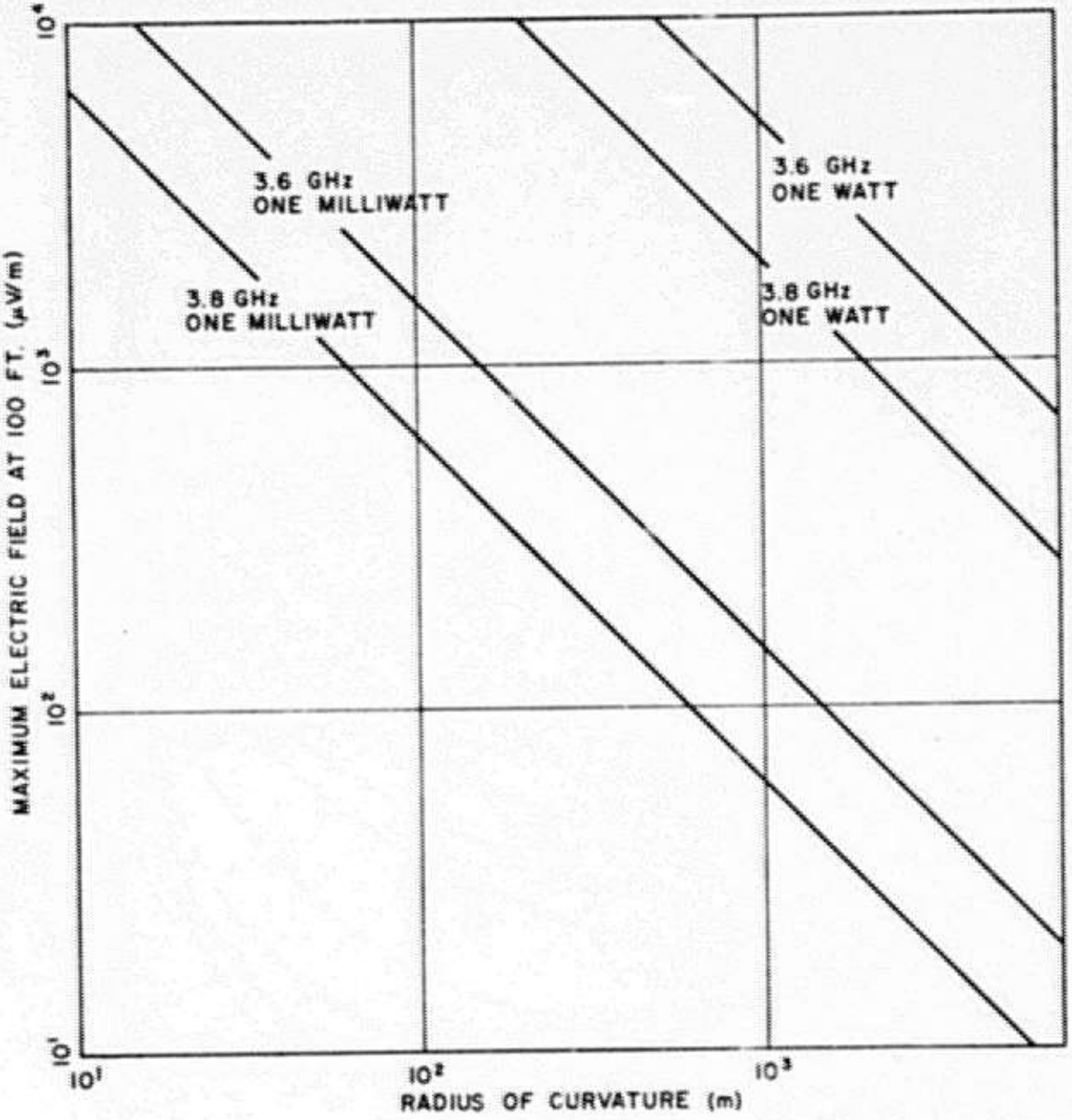

Figure 13. Electric Field at 100 Feet Resulting From a Discontinuity in Radius of Curvature

SECTION 5. PROPAGATION PROPERTIES OF A TRENCH LINE

Open dielectric waveguides have long been recognized as a promising means of achieving the large bandwidth advantages of high-frequency transmission. Many such structures have favorable attenuation characteristics and are easy to make. In contrast, conventional waveguides in fundamental mode operation have high attenuation and impractically small dimensions.

General Applied Science Labs. has studied for railroad communication applications a particular open dielectric structure consisting of a dielectric with semicircular cross-section lying in a conducting trough. Here we shall consider a possible alternate structure, consisting of a dielectric with rectangular cross-section in a trench at the bottom of a conducting trough, as shown in Figure 14. Such a structure is known to have better loss characteristics.

Our calculations take into account the fact that the waveguide must operate in a frequency region where only one mode propagates. The dispersion of the waveguide in this region will be of particular interest. Furthermore, in order to achieve low attenuation, the waveguide must operate in a region where most of the energy travels outside the dielectric, although guided by it. If it is operated so that the fields are spread too far out in space, excessive energy will be lost due to scattering from irregularities, such as curves in the waveguide.

Numerical results were obtained for the following dimensions:

a. $d/a = 4.$, $b/a = .5$

b. $d/a = 6.$, $b/a = .5$

c. $d/a = 6.$, $b/a = .333$

Only the region $3.25 < k_a < 3.75$ of case (C) was found to satisfy the requirements. In this region, the waveguide is found to be considerably more dispersive than the GASL line.

ANALYSIS

For modes propagating in the z direction, we choose an $e^{-i\omega t}$ time variation and an $e^{i\beta z}$ spatial variation. Due to the symmetry of the structure, fields of any mode will be either even or odd

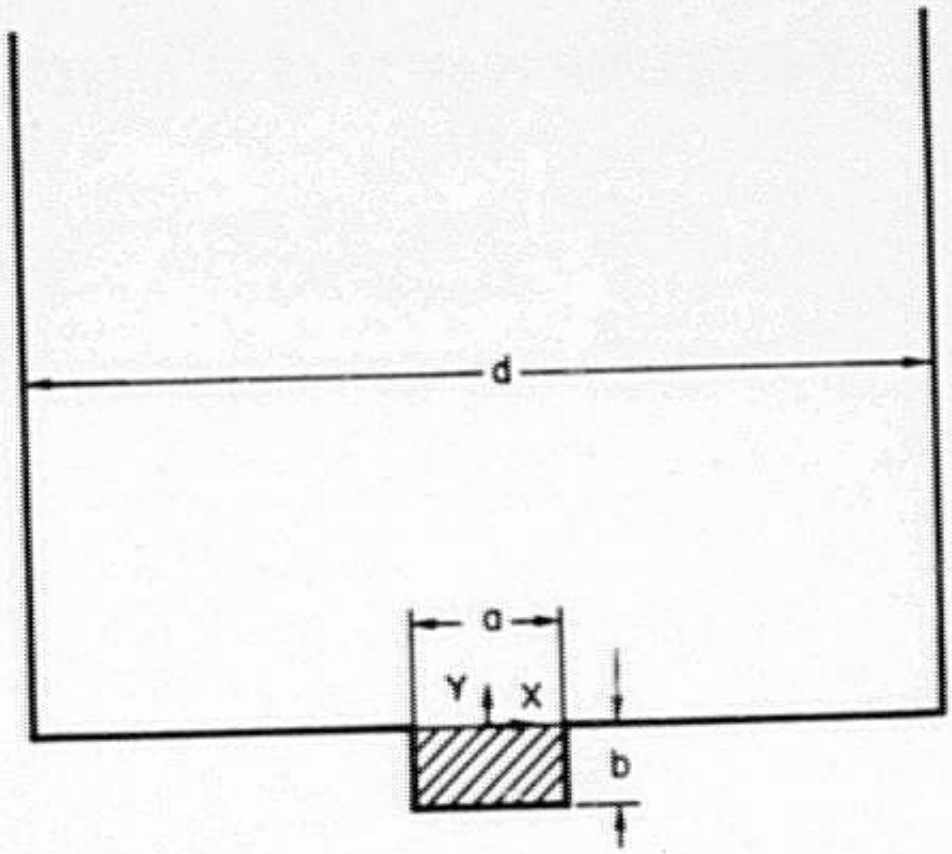

Figure 14. Cross-Section of a Trench Line

functions of x about x = 0. Consequently it is sufficient to consider only half the structure with one of the two following sets of conditions imposed:

For even modes $E_z = 0$, $E_y = 0$ } along x = 0 (an electric wall at x = 0)

For odd modes $H_x = 0$, $H_y = 0$ } along x = 0 (a magnetic wall at x = 0)

The reduced problem for even modes is shown in Figure 15a, for odd modes in Figure 15b. Since the fundamental mode is an even mode, we will give details only for this type. The analysis for odd modes is similar.

The dielectric region is denoted by I, and the air region, which extends to infinity, is denoted by II. In either region I or II, all fields can be given in terms of two components. In this case it is convenient to use H_x and H_y, which are expanded as follows:

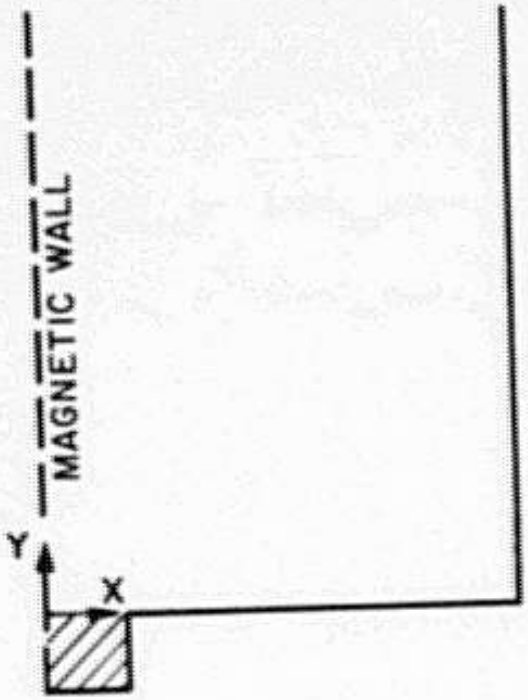

Figure 15a. Reduced Problem for Even Modes

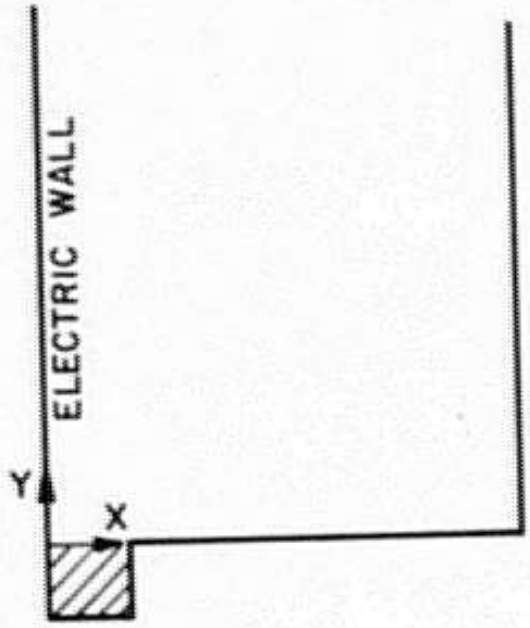

Figure 15b. Reduced Problem for Odd Modes

Region I:

$$H_x = \sum_n A_n \cos p_n x \cosh q_n (y+b) \tag{28a}$$

$$H_y = \sum_n B_n \sin p_n x \sinh q_n (y+b) \tag{28b}$$

Region II:

$$H_x = \sum_n C_n \cos p_{on} x \exp(-q_{on} y) \tag{29a}$$

$$H_y = \sum_n D_n \sin p_{on} x \exp(-q_{on} y) \tag{29b}$$

where

$$p_n = 2(n-1)\pi/a$$

$$q_n = \beta^2 - k^2\kappa + p_n^2$$

$$p_{on} = 2(n-1)\pi/d$$

$$q_{on} = \beta^2 - k^2 + p_{on}^2$$

$$k^2 = \omega^2 \mu_o \varepsilon_o$$

κ = relative dielectric constant

These expansions are complete if the summations over n go from one to infinity. However, for computational purposes, the infinite summations are truncated to a finite number of terms, specifically N_1 for eq. (28a,b) and N_2 for eq. (29a,b). Arbitrarily good results can be obtained by taking N_1 and N_2 sufficiently large.

The other field components can each be expressed in terms of H_x and H_y through Maxwell's equations. The resulting expressions are complete and satisfy the wave equation in their appropriate regions. Further, they satisfy all boundary conditions except those at y = 0.

$$E_x(x,0+) = \begin{cases} E_x(x,0-) & \text{for } 0<x<\frac{a}{2} \\ 0 & \text{for } \frac{a}{2}<x<\frac{d}{2} \end{cases} \tag{30}$$

$$E_z(x,0+) = \begin{cases} E_z(x,0-) & \text{for } 0<x<\frac{a}{2} \\ 0 & \text{for } \frac{a}{2}<x<\frac{d}{2} \end{cases} \tag{31}$$

$$H_x(x,0+) = H_x(x,0-) \qquad \text{for } 0<x<\frac{a}{2} \tag{32}$$

$$H_z(x,0+) = H_z(x,0-) \qquad \text{for } 0<x<\frac{a}{2} \tag{33}$$

When these are written in terms of the previous expansions, the orthonormal properties of the trigonometric functions may be used to obtain the following results:

$$\kappa dp_{om}q_{om}C_m+\kappa d(p_{om}^2-\kappa^2)D_m = -4\sum_n p_n q_n \sinh(q_n b)\alpha_{mn}A_n + 4\sum_n (p_n^2-k^2\kappa)\sinh(q_n b)\alpha_{mn}B_n \tag{34}$$

$$\kappa dq_{om}C_m+\kappa dp_{om}D_m = -4\sum_n q_n \sinh(q_n b)\gamma_{mn}A_n + 4\sum_n p_n \sinh(q_n b)\gamma_{mn}B_n \tag{35}$$

$$4\sum_n \gamma_{nm}C_n = \cosh(q_m b)A_m \tag{36}$$

$$4\sum_n p_n \alpha_{nm}C_n+4\sum_n q_{on}\alpha_{nm}D_n = +p_m\cosh(Q_m b)A_m + q_m\cosh(q_m b)B_m \tag{37}$$

where

$$\alpha_{mn} = \int_0^{a/2} \sin p_{om}x \sin p_n x\,dx$$

$$\gamma_{mn} = \int_0^{a/2} \cos p_{om}x \cos p_n x\,dx$$

By retaining N_2 terms in (11) and (12) and N_1 terms in (36) and (37), we obtain the $2N_1 + 2N_2$ equations needed to determine the unknown coefficients: A_1,-----A_{N_1} B_1--B_{N_1}, C_1--C_{N_2}, D_1---D_{N_2}. In order for a solution to exist, the determinant of the coefficients, Δ, must vanish. Since Δ is a function of β^2, we have

$$\Delta(\beta^2) = 0 \tag{38}$$

That is, values of β which cause Δ to vanish represent the propagation constants of non-radiating modes.

Upper and lower bounds on β^2 can be established which specify the region in which solutions to eq. (15) should be sought. These are given by

$$\omega^2\mu_o\varepsilon_o\kappa > \beta^2 > \max\left\{\begin{matrix} 0 \\ k^2 - (\pi/c)^2 \end{matrix}\right\}$$

Once β has been determined, the $|A_n|$, $|B_n|$, $|C_n|$, $|D_n|$ are readily computed from eq. (11)-(14), providing knowledge of the field structure.

NUMERICAL RESULTS AND CONCLUSIONS

With $\kappa = 2.56$ and all distances normalized to the trench-width, a, the following waveguide dimensions were chosen for computations:

a. $d/a = 4.$, $b/a = .5$

b. $d/a = 6.$, $b/a = .5$

c. $d/a = 6.$, $b/a = .333$

In most cases the truncation $N_1 = 2$ and $N_2 = 5$ gave good results That is, increasing N_1 or N_2 did not significantly affect the answer. This resulted in 14x14 matrices ($2N_1+2N_2=14$).

The propagation characteristics were computed as a function of frequency for dimensions (A.), (B.) and (C.). The results, expressed as $c/v_p = \beta a/ka$ vs. ka, are given in Figures 17, 18, and 19 respectively. The mode with the lowest cutoff frequency, i.e., the fundamental mode, is an even mode with electric fields as shown in Figure 16. The next lowest cutoff frequency also belongs to an even mode. Since it ir desired that only one mode propagate, any useful frequency region must be between these two cutoff frequencies.

The c/v_p vs. ka diagrams (dispersion curves) of the fundamental mode exhibit two distinct regions separated by an inflection point which lies between ka = 2.2 and ka = 2.5. Below this point virtually all energy lies outside the dielectric and the rate of field decay in the y-direction is quite small. As one might expect, the propagation constant is very nearly that for a parallel-plate waveguide, i.e.,

$$(\beta a)^2 = (ka)^2 - (\pi a/c)^2$$

In the region above the inflection point, the field decays in the y-direction, and the propagation characteristics depart from those of a parallel-plate waveguide. In this region, changing d/a from 4. to 6. with b/a = .5 (Figures 17 and 18), reduces the dispersion. Figures 18 and 19 show that changing b/a from .5 to .333, with d/a = 6., has a similar effect.

Figures 17 and 18 indicate that the propagation characteristics of the first even mode are little affected by d/a. However, figures 18 and 19 suggest that this mode is very sensitive to changes in b/a. The cutoff frequency is increased considerably when b/a is changed from .5 to .333, with d/a = 6.

As y becomes large the fields of the fundamental mode decrease as $\exp-(q_{o1}/a)y$. Figure 20 gives q_{o1}/a as a function of ka.

Figure 21 displays the percent of the total power carried in the dielectric as a function of ka. The attenuation due to dielectric loss is proportional to this fraction of the power.

With the GASL results in mind, we wish to select a frequency region in which 2% to 6% of the energy lies within the dielectric and only the fundamental mode propagates. Of the three cases studied, only case (c) exhibits such a region - namely $3.25 < ka < 3.75$.

In order that the dispersion in this region may be compared to that of the GASL line, we present the following figures of merit.

	Imbedded rectangular dielectric	GASL Line
$\frac{d(c/v_p)}{df}$	$.5\,(\text{GHz})^{-1}$ for a = 2cm	$.02\ (\text{GHz})^{-1}$
$\frac{d^2(c/v_p)}{df^2}$	$.1\ (\text{GHz})^{-2}$ for a = 2cm	$.02\ (\text{GHz})^{-2}$

It is seen that the dielectric waveguide examined here, is more dispersive in the region considered than the GASL line. For wideband operation this disadvantage outweighs the advantage of lower losses.

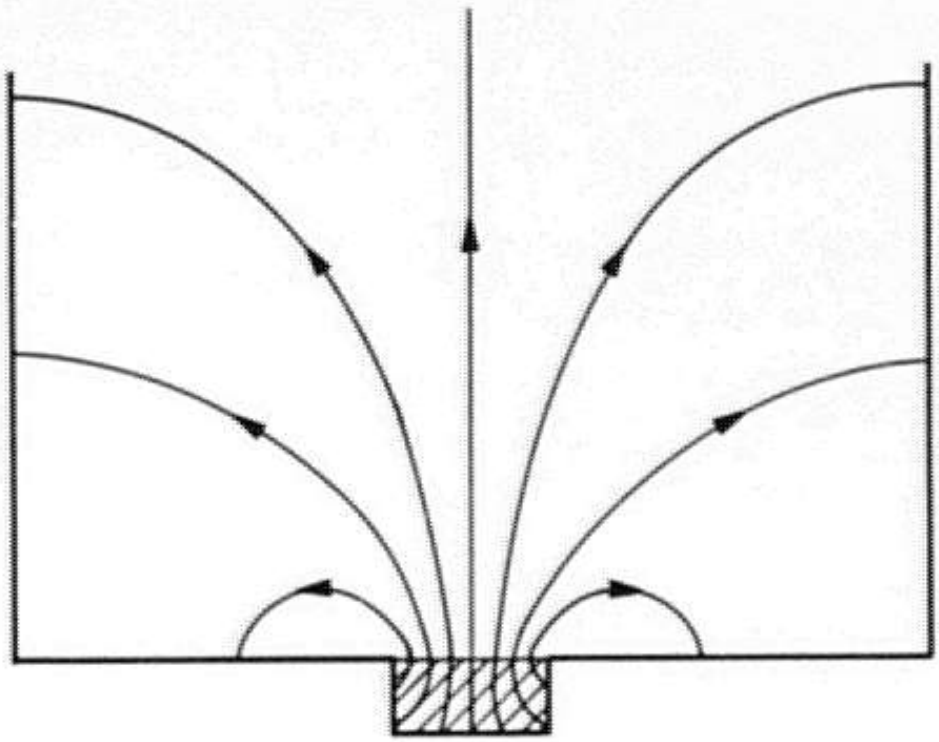

Figure 16. Electric Field Configuration of the Fundamental Mode

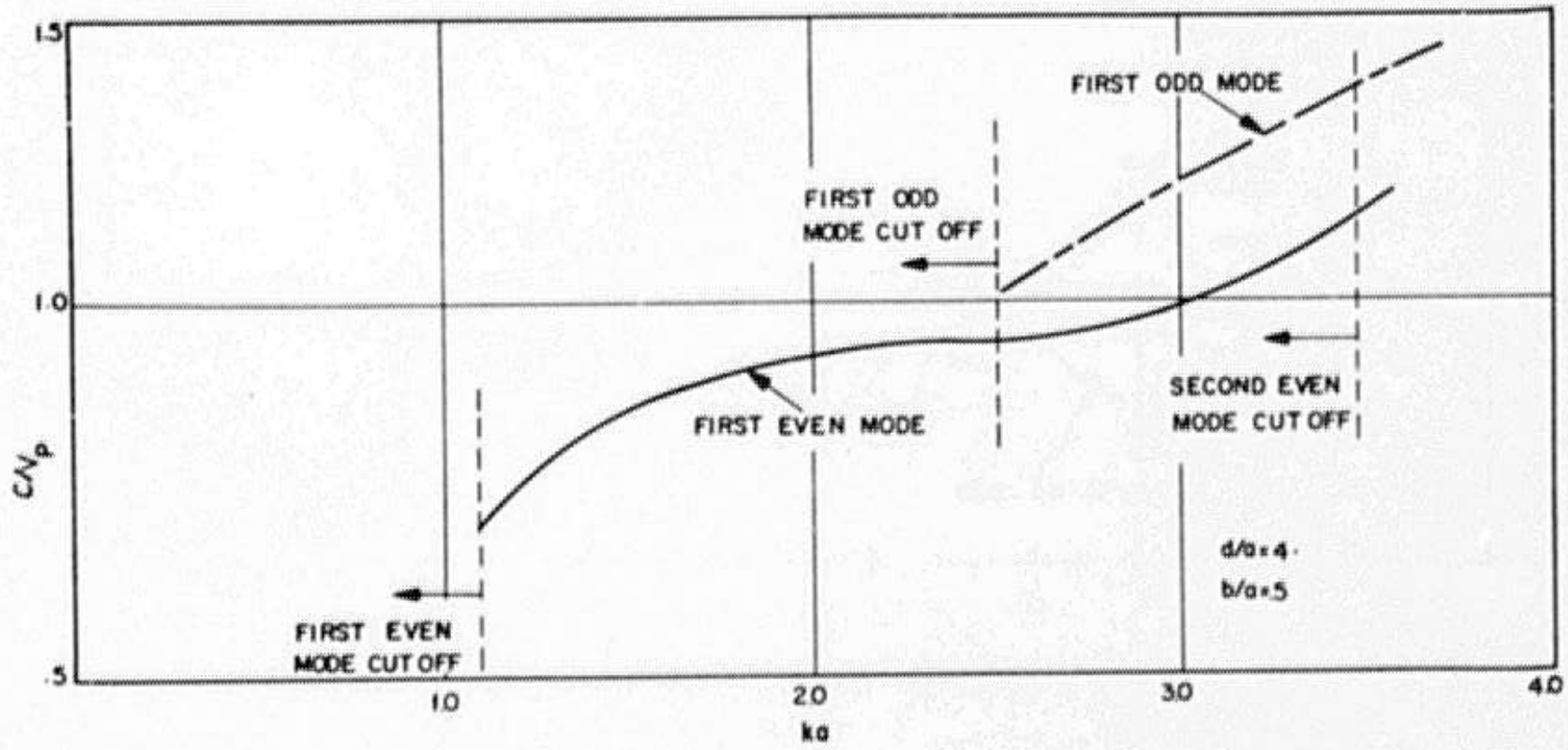

Figure 17. Propagation Characteristics for d/a = 4. and b/a = .5

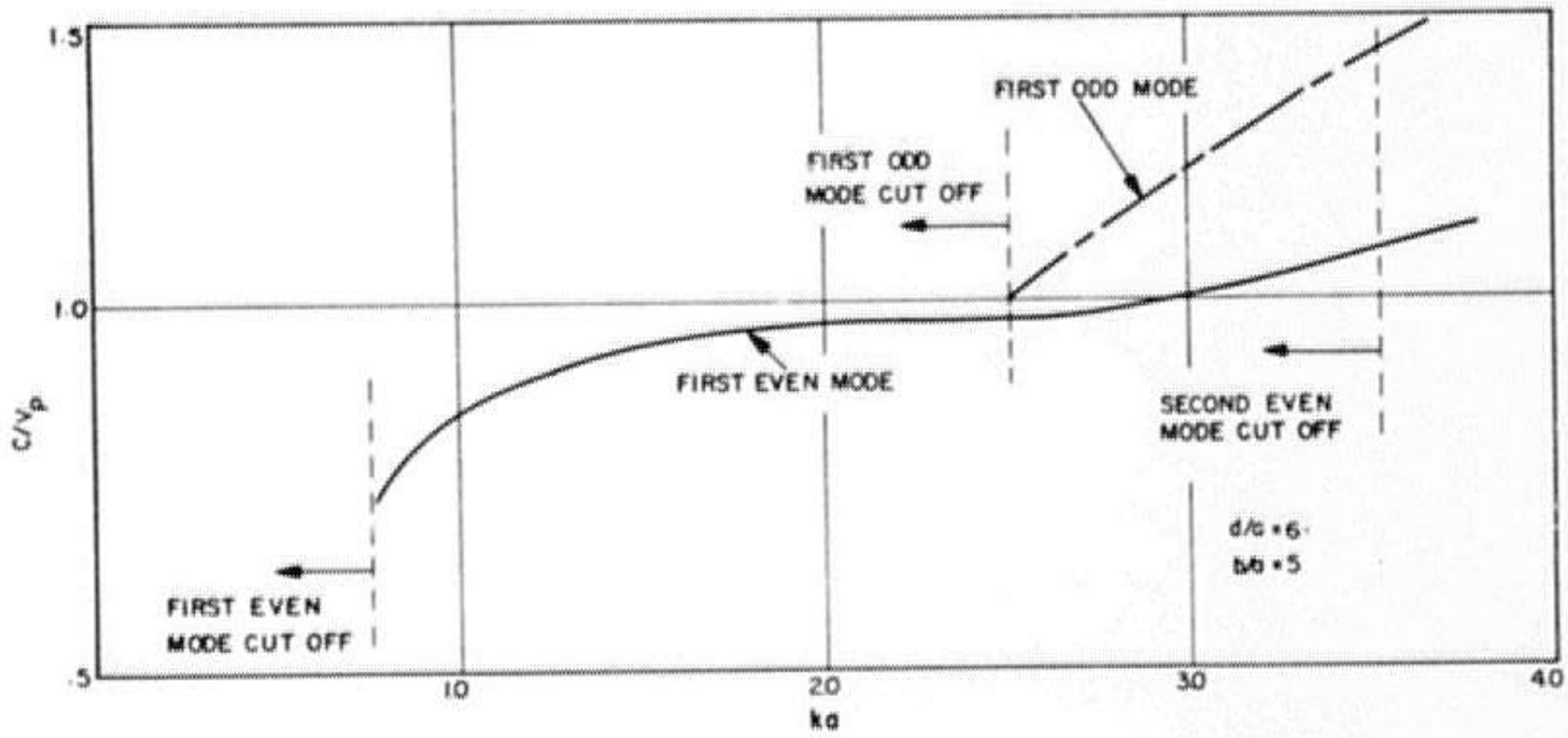

Figure 18. Propagation Characteristics for d/a = 6. and b/a = .5

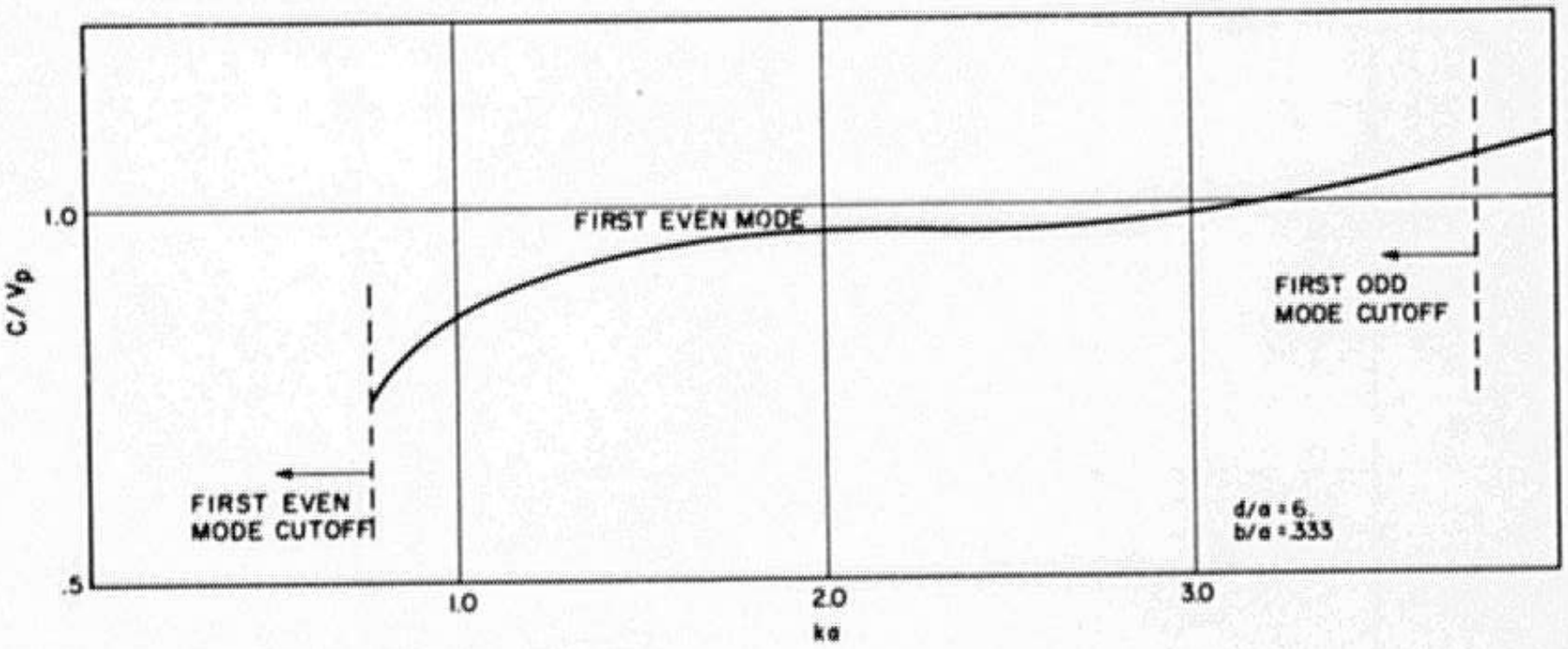

Figure 19. Propagation Characteristics for d/a = 6. and b/a = .333

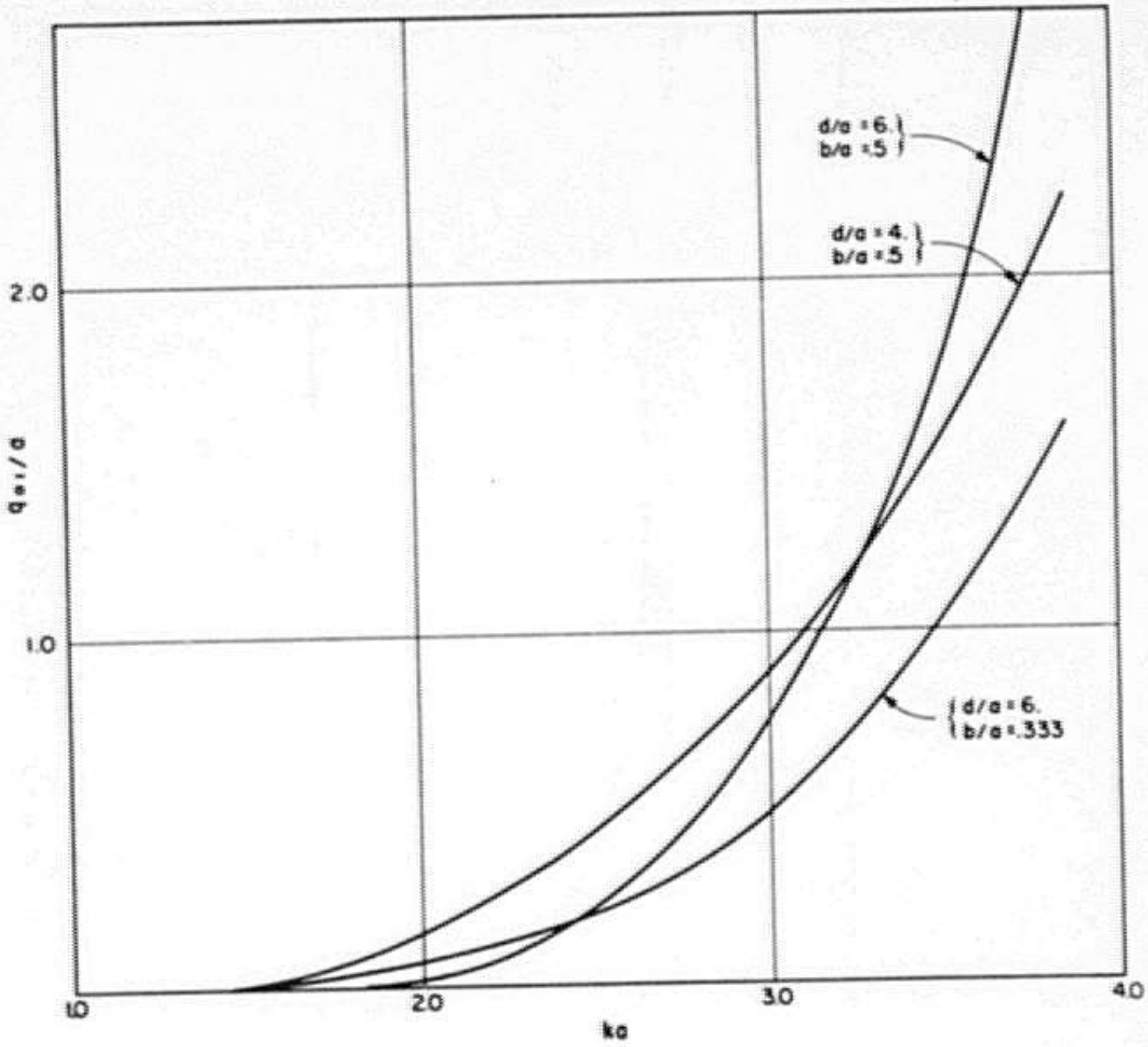

Figure 20. Rate of Field Decay Away from the Dielectric

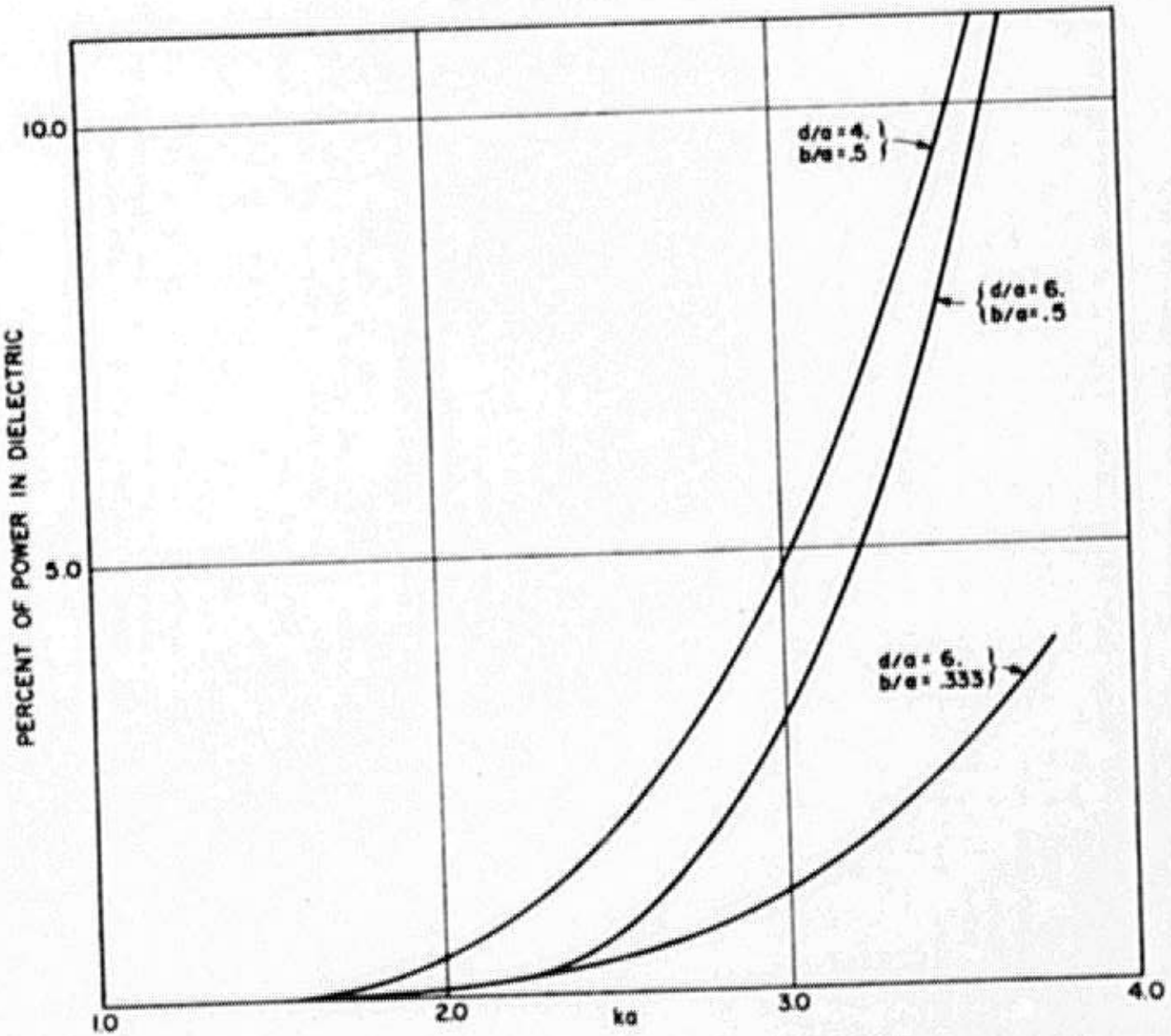

Figure 21. Percent of Total Power Carried in the Dielectric

SECTION 6.

PCM AND COMMUNICATIONS FOR HIGH SPEED GROUND TRANSPORTATION

Two aspects of long-distance communications with high-speed ground vehicles over microwave transmission lines make pulse code modulation techniques seem attractive. First, the reliability of the command and control system demands all the advantages of PCM - immunity to interference, maintenance of transmission quality over long distances, and the use of regenerative repeaters. Second, the non-uniform frequency response of long transmission lines with its characteristic ripple distortion produces unacceptable degradation in signals that use uncoded modulation such as FM. The increased bit error rate for PCM produced by this distortion is not serious, however, and to a certain extent can be compensated, as will be shown below. We shall begin by reviewing PCM techniques.

GENERAL CHARACTERISTICS

Pulse code modulation is a pulsed carrier system that transmits discrete samples of a signal that is a continuous function of time. Each sample is approximated by the nearest of a selected number of discrete (quantized) values, and each value is assigned a particular pulse code pattern uniquely related to the magnitude of the quantized sample. Representing a sampled value of the signal in this way introduces an initial amplitude error and gives rise to quantization noise. Once the signal has been quantized and coded, however, it can be relayed many times without further degradation, provided only that the added noise in the signal presented to each repeater is not too great to prevent recognition of the particular code which represents the sample. As stated above, each quantized sample is transformed before transmission into a code of n-pulses. The number of pulses-per-sample depends on the number of quantization levels and the basis of the code. For example, the binary code for 8-level quantization requires three pulses-per-sample (minimum for intelligible speech), while the same code for 128-level quantization requires 7-pulses (high quality telephony). In general, the number of quantization levels is given by

$$M = 2^n .$$

Changing the number of quantization levels M has a direct effect on the bandwidth requirements and the quantization signal-to-noise ratio. The sampling theorem states that if a signal wave whose highest frequency component is f_m is sampled at the

rate of $2f_m$ samples per second, a suitable receiver will restore the signal wave from the samples. With n pulses per sample, the minimum bandwidth required is $2nf_m$. Thus, 8-level quantization of a 5-KHz signal requires a safe minimum of 60-KHz with double side-band modulation; 128-level quantization of the same signal would require at least 140-KHz of bandwidth. On the other hand, the quantization S/N ratio is greatly increased. Expressed in dB, it is

$$D = 20 \log M .$$

For an 8-level code the ratio is 18-dB; for 128-levels it is 42-dB.

In every transmission system there is an accumulation of noise and distortion that increases with the length of the system. A major advantage of PCM is that it is possible to remove these impairments by means of regenerative repeaters. In contrast to ordinary repeaters, which amplify both signal and noise alike, a regenerative repeater replaces the misshapen and noisy received pulses with properly formed, standard pulses, free of noise. It is only necessary that the received pulses still be recognizable. Figure 22 shows the input carrier-to-noise ratio required for an output S/N of 60-dB as a function of the number of repeaters on the line. It is seen that for 50 non-regenerative repeaters the carrier-to-noise ratio must be increased about 17-dB, while for regenerative repeaters the required increase is only 1-dB.

DIGITAL MODULATION TECHNIQUES – PSK

PCM codes may be used to modulate a radio frequency carrier in various ways. Three common modes are amplitude-shift keying (ASK), frequency-shift keying (FSK) and phase-shift keying (PSK). In ASK the carrier amplitude is changed in accordance with the level of the code symbol. For example, with a binary basis the two states in an n pulse code may be represented by the presence or absence of the carrier. In FSK the pulse information is transmitted by the sequential transmission of carrier pulses of constant amplitude but different frequencies. In PSK the carrier pulses of constant amplitude and frequency have different relative phases. In general, digital transmission using phase-shift keying is less sensitive to noise than either frequency or amplitude-shift keying.

Any of these keyed signals may be processed by either coherent or non-coherent detection systems. For a given modulation technique the same probability of error can be achieved with less power using coherent detection. With coherent PSK a pilot signal is generally transmitted along with the carrier to serve as a phase reference which permits the

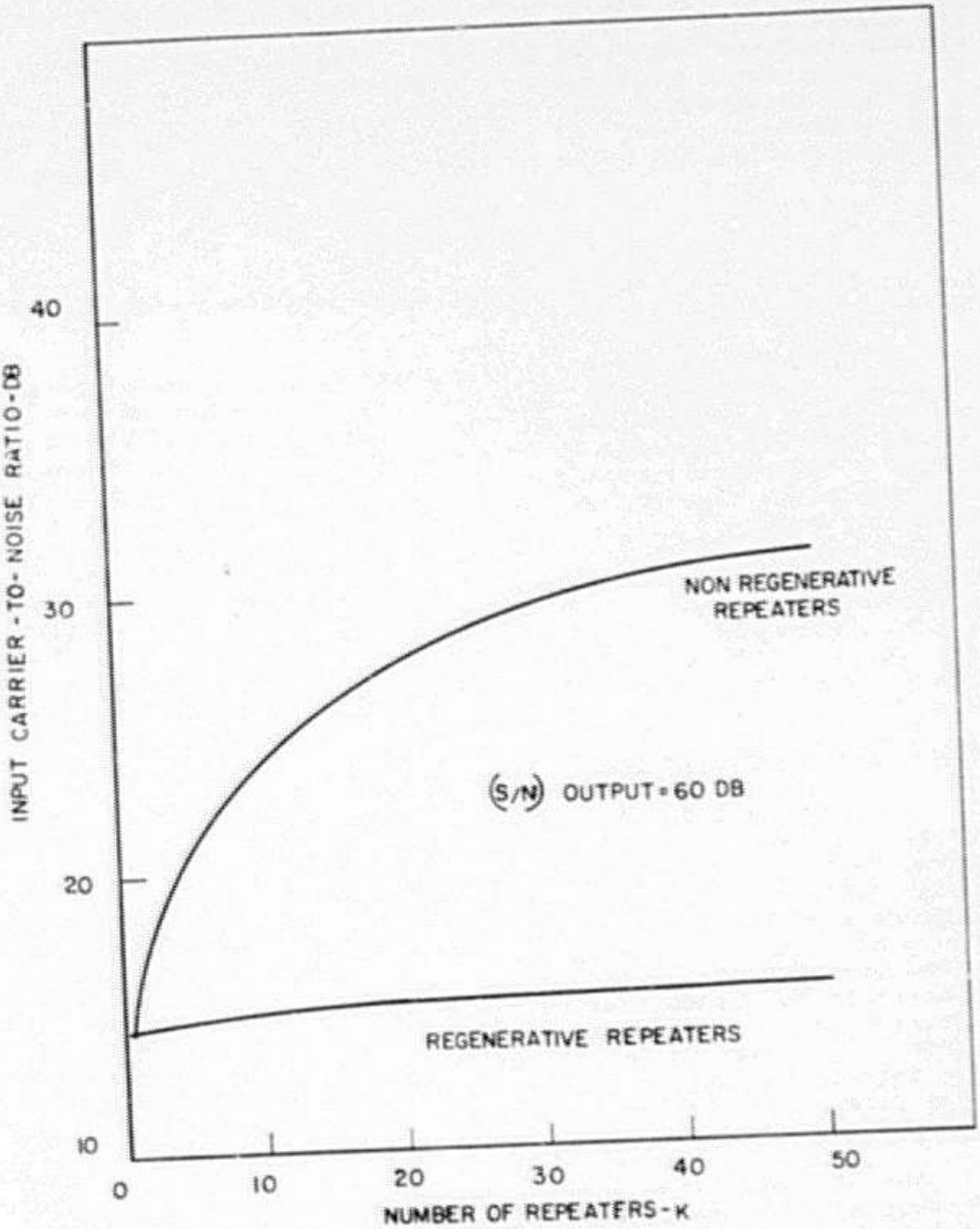

Figure 22. Input Signal-to-Noise Ratio vs. Number of Repeaters for Constant Output Signal-to-Noise Ratio.

receiver to be phase locked to the transmitter. When this is not feasible a "differentially coherent" system may be used in which the code level is translated into the relative (instead of the absolute) phase of adjacent signal elements. In the detection process a received element is held and used as a reference to be compared with the succeeding element. Figures 23 and 24 compare the bit error probability for coherent and incoherent systems for all modulation modes. Note that at the higher signal energies ($E/N_o \sim 3dB$) the energy requirement for coherent PSK is 3 dB less than for coherent FSK with the same probability of error. In Figure 25 differentially coherent and coherent PSK are compared. It is seen that for a binary system ($m = 2$) the degradation approaches zero and rises to a maximum of 3 dB as the number of phases is increased.

In all pulse coded systems, when the signal energy-to-noise ratio exceeds a certain threshold, the probability of error decreases exponentially. This is shown by the formulas that have been derived for binary PSK:

Coherent:

$$P_e = \operatorname{erfc}(2E/N_o)^{1/2}$$

$$= \left[\left(1-1/(2E/N_o)\right) \; /2(\pi E/N_o)^{1/2}\right] \quad \exp(-E/N_o), \; E/N_o > 2$$

Diff. Coherent: $P_e = (1/2)\exp(-E/N_o)$

The ratio, E/N_o, is a convenient parameter for comparing different digital modulation methods. It is often denoted by a figure of merit β and represents the ratio of the signal energy required per bit to the noise power spectral density in watts per cycle for a given error. Typical curves are given in Figures 26, 27 and 28.

BANDWIDTH REQUIREMENTS

Considerable experience has been accumulated in the use of PCM for telephony. For example, the Bell Telephone Laboratories has built a binary PCM system in which the code pulses of 12 telephone circuits are interlaced by time division multiplexing. Groups of 12 circuits each group amplitude keying (ASK) its own carrier are assembled on a frequency division multiplex basis. This system requires a transmission bandwidth of 1.5-MHz

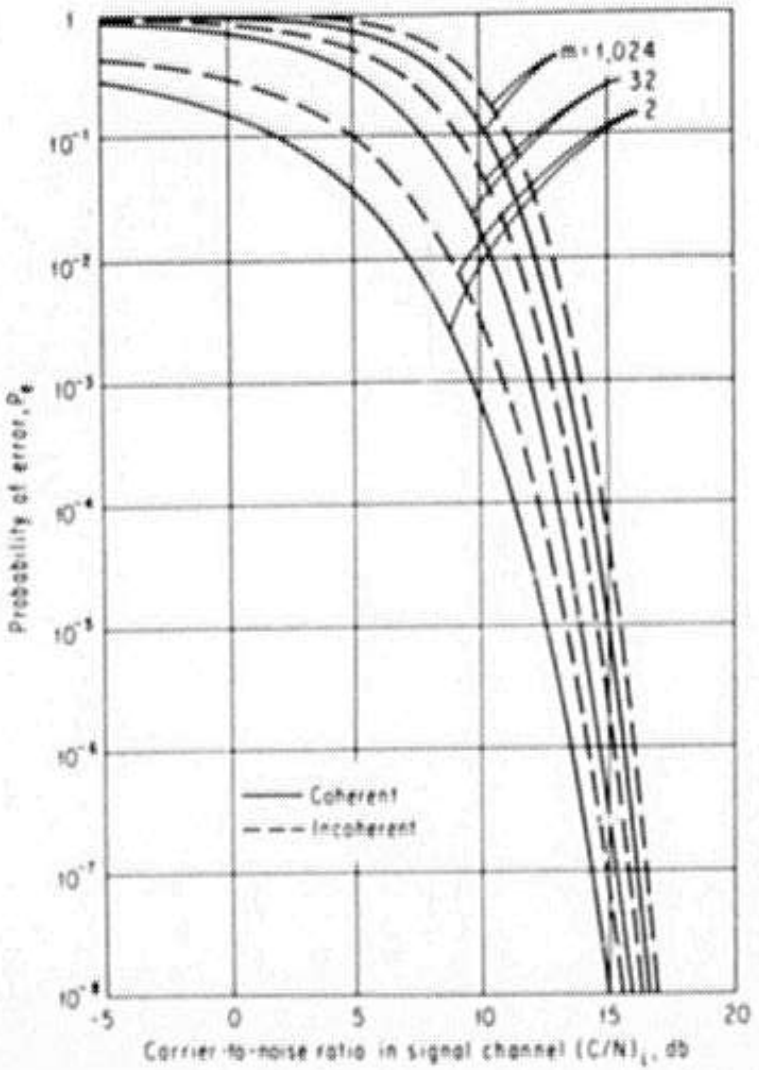

Figure 23. A Comparison of Probability of Error Between Coherent and Noncoherent Multiple PSK Systems. (From Akima(8), Natl. Bur. Standards.)

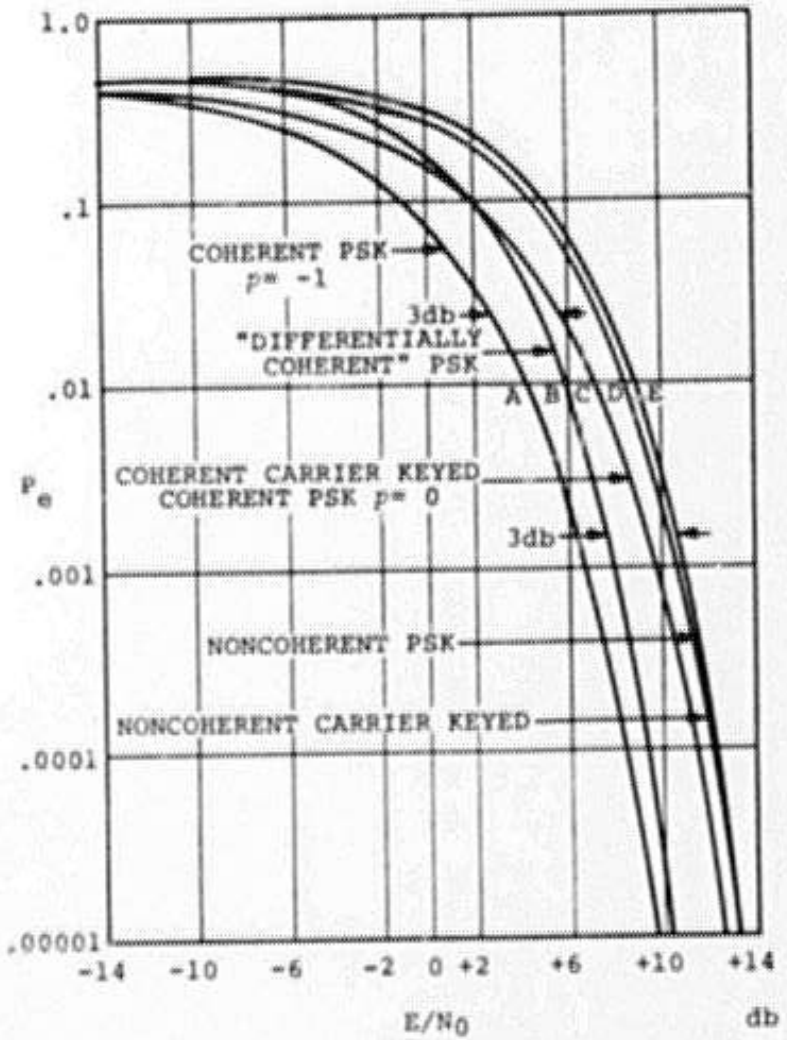

Figure 24. Probability of Error vs. Signal Energy/Noise Power Density. (From Lawton(10), Proc. 2d Natl. Conf. Military Electron.)

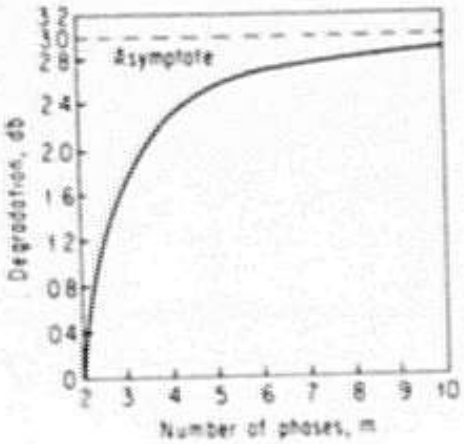

Figure 25. Degradation of Phase-Comparison Detection Compared to Coherent Phase Detection. (From Cahn (11), IRE Trans. Commun. Systems.)

for each group of 12 circuits, that is, 125-kHz per circuit. The same bandwidth has been proposed by the Bell Labs for a satellite communications system using PCM-PSK. For a two-phase system at 125-kHz per circuit this gives 16,000 voice grade circuits in a 2-GHz band between 18 and 20-GHz; for a four-phase system the required bandwidth is halved to 62.5-kHz per circuit providing 32,000 voice circuits in the same rf band but with 2-dB degradation. The same system uses 6.25-MHz for a video-phone circuit and 83-MHz per TV circuit.

With these numbers one can calculate the bandwidth needed for various communications functions between wayside and vehicle. These are shown in Table I. It is noteworthy that one TV channel occupies more bandwidth than 1,000 high quality voice circuits. One might try to reduce this requirement by techniques similar to those proposed for CATV, but the gains are marginal at best. A similar solution would be to carry video taped TV programs on the vehicle, which would not only cut the total bandwidth in half but also remove a major problem associated with the multiple reflections that occur in any long transmission line.

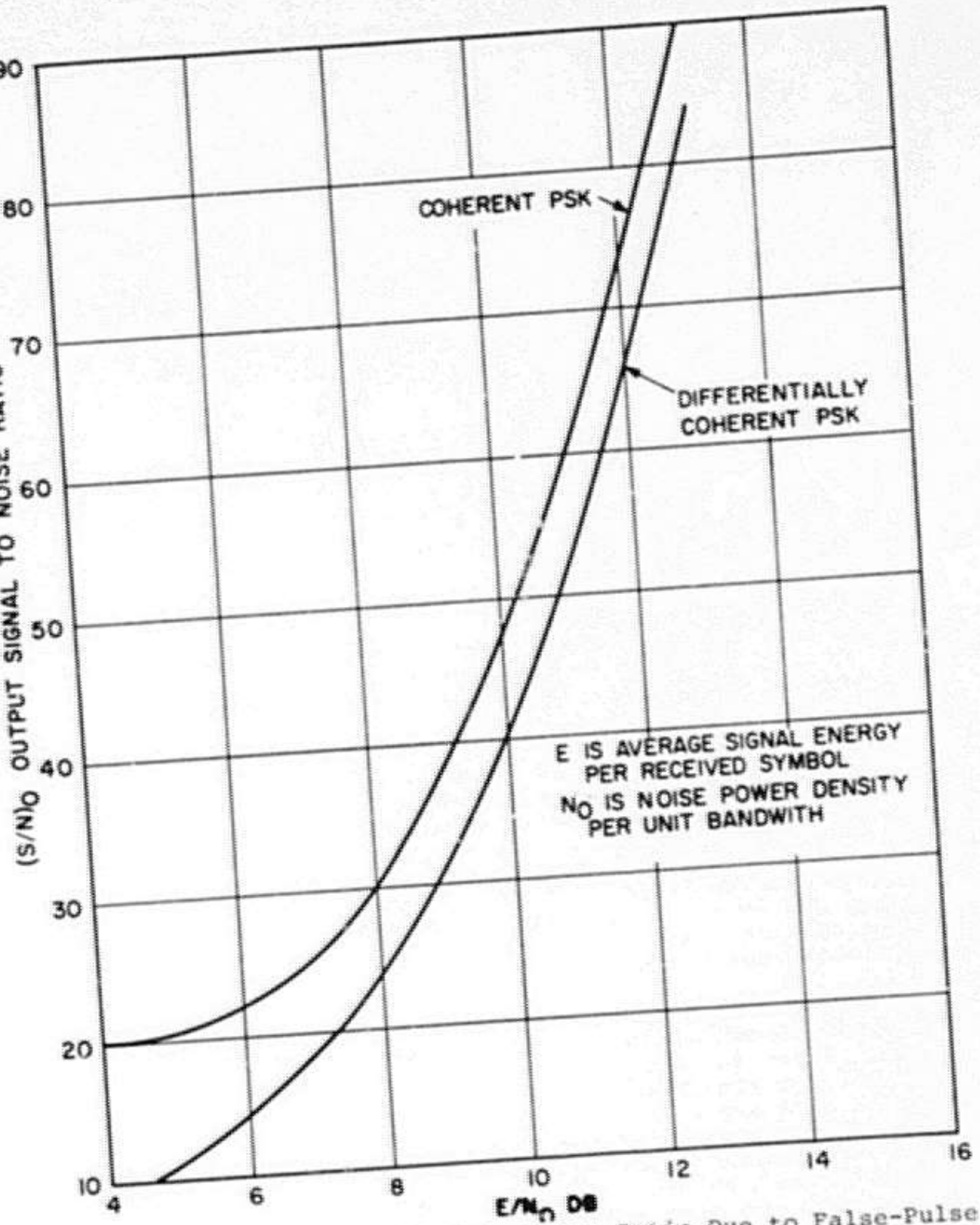

Figure 26. Output Signal-to-Noise Ratio Due to False-Pulse Noise vs. Signal Energy-to-Noise Power Density Ratio Binary PSK.

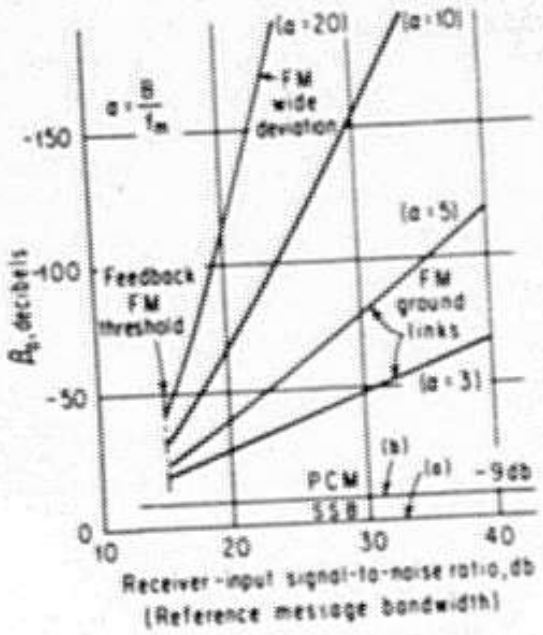

Figure 27. Efficiencies of Various Modulation Systems (From Wright and Jolliffee (12), J. Brit. IRE.)

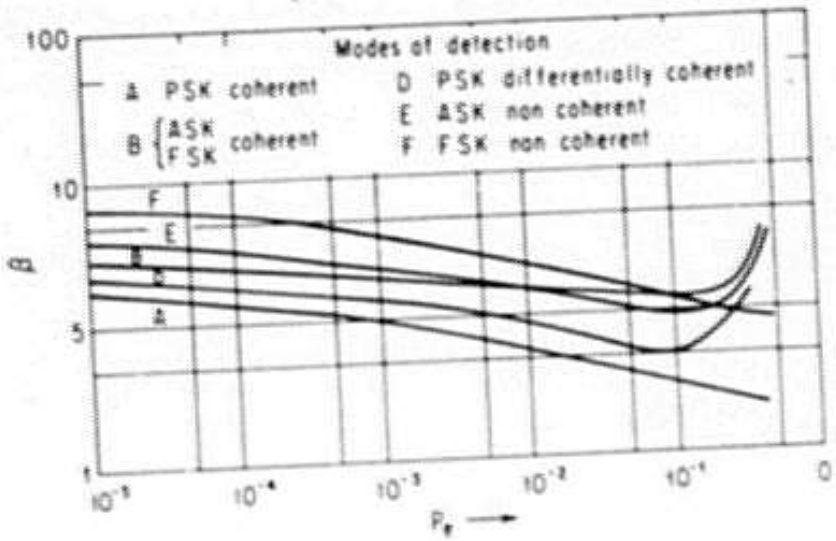

Figure 28. Comparison of Various Binary PCM Systems on a β Factor Basis. (From Hancock (13), Proc. Natl. Electron. Conf.)

PCM ON LONG LINES WITH NON-UNIFORM TRANSMISSION CHARACTERISTICS

For an ideal uniform, non-dispersive transmission line, the bandwidth limitations are set only by the associated circuitry and coupling devices. In practice, however, the line is dispersive and does produce internal reflections at bends, joints and couplers as well as at the periodic and random non-uniformities that are inevitably introduced during manufacture and installation. These reflections are not consequential for short distances, but over many miles they can add up to a transfer function with deep absorption spikes between which are amplitude and phase rippler of smaller amplitude. A typical example, as computed at New Mexico State University, is shown in Figure 29.

The frequency interval Δf between absorption spikes is set by the distance between the regularly spaced reflection points according to the formula

$$\Delta f = c/2L$$

where c is the speed of light on the line. To avoid these absorption spikes it is possible to group the audio channels into bands that fall between them. Since these clear bands are not likely to exceed 15 MHz in width (corresponding to a minimum spacing of 10-meters between reflection points), such a solution will not work for TV unless some kind of frequency division can be devised which will not suffer from the dispersive propagation characteristic of the line. A solution along these lines would be expensive and complicated. It might well prove more advantageous to try to squeeze a frequency modulated TV signal between the spikes, but this will require the regularly-spaced reflection points on the transmission line to be no more than 10-meters apart, which might be difficult to achieve.

Between the absorption spikes of Figure 29 the transfer function exhibits quasi-periodic ripples which are the result of random variations in the length of the transmission line segments. These ripples produce pulse echoes (false pulses) in a PCM system and lead to higher bit error rates. The general problem cannot be handled analytically, but can be formulated in terms of a transfer function of the form

$$T(\omega) = A(\omega) \exp\left\{j\Phi(\omega)\right\}$$

If the spectrum of the original signal, s(t), is $S(\omega)$, the distorted signal has the representation

$$s_d(t) = (1/2\pi) \int_{-\infty}^{\infty} S(\omega)T(\omega)e^{j\omega t}d\omega.$$

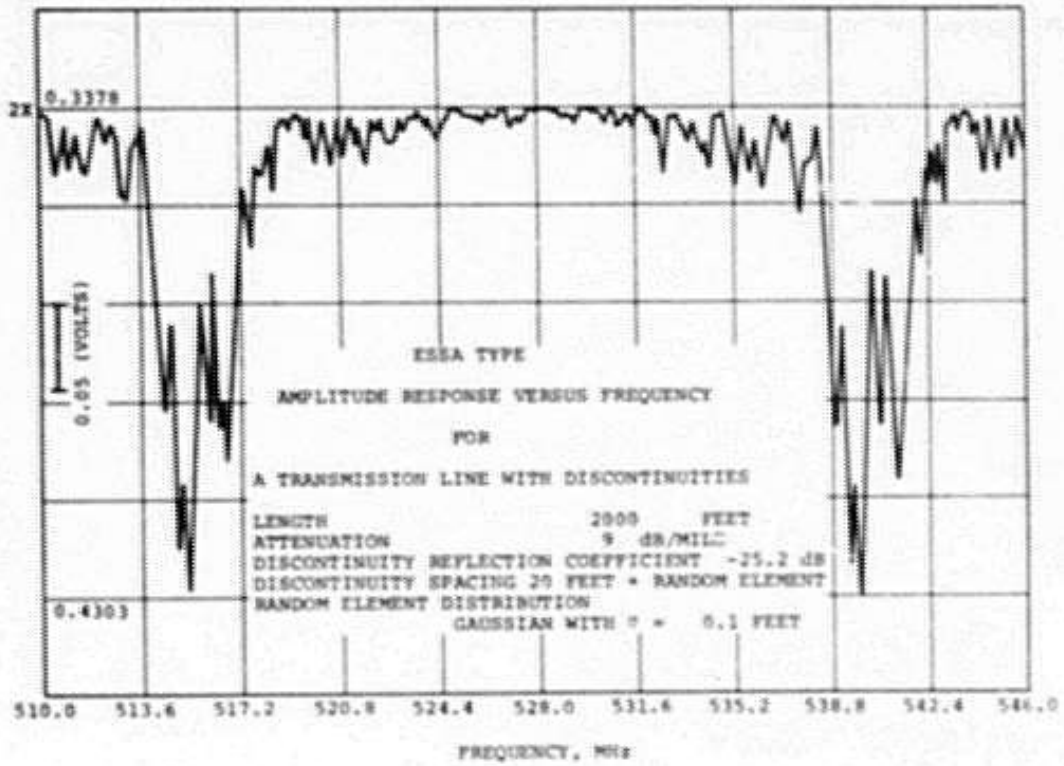

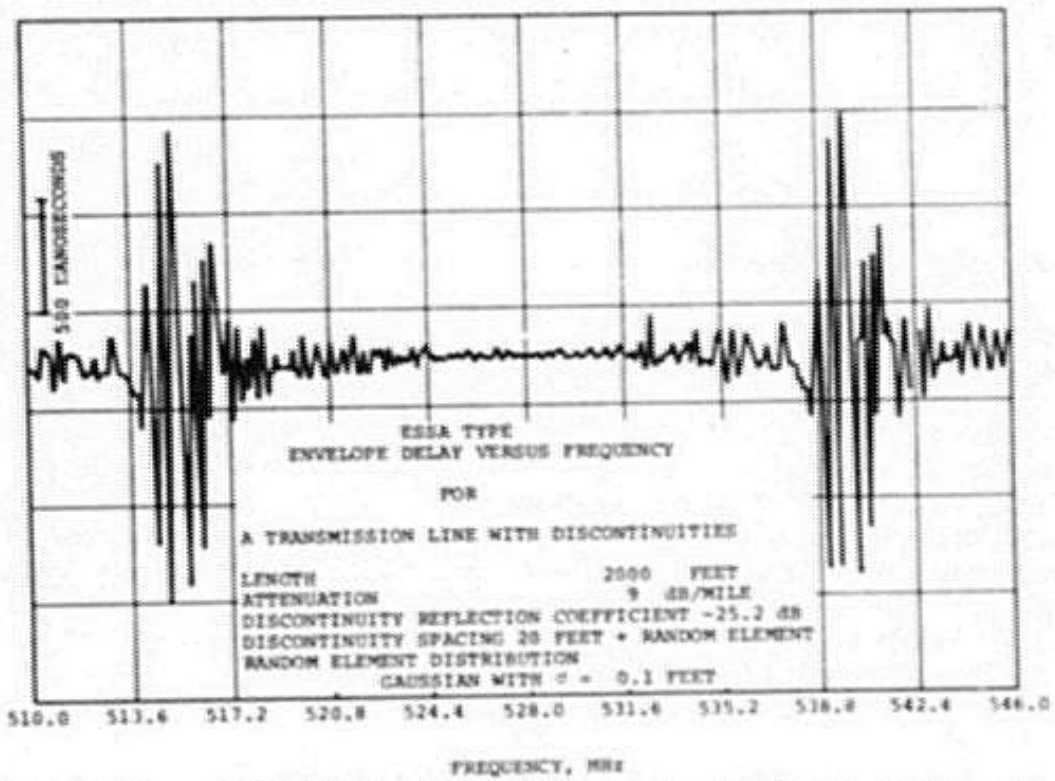

Figure 29. Amplitude Response and Envelope Delay vs. Frequency for a Transmission Line with Reflection Discontinuities. (From a Report of the Physical Science Lab., New Mexico State Univ. (14))

A simple model for $T(\omega)$ that is widely used for analytical study is

$$A(\omega) = (a_o/2) + a_1 \cos\omega\tau$$

$$\Phi(\omega) = -b_o\omega + b_1 \sin\omega\tau$$

These functions agree fairly well with the smoothed responses calculated at New Mexico. When they are substituted together with an input pulse spectrum into the formula for the distorted signal, the integral can be expressed as a series of pulses including the undistorted original plus advanced and delayed pulses of identical shape but diminishing amplitude, often called "echoes". The original pulse is reduced in amplitude by the factor $a_o/2$ and delayed in time by b_o seconds. The echoes are separated from the original by integral multiples of τ seconds.

For $b_1 << 1$ all echoes beyond the first may be neglected and the distorted pulse is simply

$$s_d(t + b_o) = (a_o/2)\, J_o(b_1)\, s(t) + \left[(a_o/2)J_1(b_1) + (a_1/2)J_o(b_1)\right] s(t + \tau) + \left[(a_1/2)J_o(b_1) - (a_o/2)J_1(b_1)\right] s(t - \tau)$$

where J_o and J_1 are Bessel functions of the first kind.

With binary coherent PSK the actual input signal is a string of code pulses each of which may have one of two possible phases differing by π radians. On a transmission line with the kind of ripple distortion described above the time interval occupied by any one of these pulses will also include echo pulses of smaller amplitude from code pulses occupying other intervals in the string. These false pulses increase the bit error probability. In order to calculate the effect only the worst case will be considered. This will occur when two echoes fall exactly into the pulse interval and have phases opposite to that of the code pulse. The probability of error then becomes

$$P_e = \text{erfc}\left[F(2E_o/N_o)^{1/2}\right]$$

where

$$F = J_o(b_1) - |J_1(b_1) + (a_1/a_o)J_o(b_1)|$$

$$- |J_1(b_1) - (a_1/a_o)J_o(b_1)|$$

For a uniform line $a_1 = b_1 = 0$, $F = 1$, and P_e is the same as that previously given. Otherwise $F < 1$, and the bit error rate is increased. This is shown in Figures 30 and 31 for two different E/N_o ratios, assuming that the amplitude and phase effects are equal.

It should be noted that the factor F is independent of the undistorted pulse amplitude. This fact makes it possible to reduce the error probability by increasing the energy of the signal pulse even in the presence of ripple distortion. Thus, if the energy is increased to E_1 so that

$$E_1/E_o = 1/F^2$$

the increased error probability is exactly compensated. The required increase is plotted in Figure 32 as a function of the ripple amplitude. Since higher order echoes are not included, the curve represents a lower bound.

Calculations based on data in the New Mexico report (Table 5) indicate that for the examples used there, the required energy increase is not very great. Two of these examples for lines one mile long are summarized below.

	Discontinuity		Ripple	Diff. Delay	
Case No.	Refl. Coeff.	Spacing	Amplitude	ns	E_1/E_o
5 (ESSA)*	-25.2 dB	20±0.1 ft.	1.5 dB	277	1.21
18 (GASL)**	-40.0 dB	20±0.025 ft.	0.5 dB	181	1.07

*0.5 GHz **8.0 GHz

CONCLUSIONS

PCM is a wide band modulation scheme that trades bandwidth for reliability. That is, it offers high signal-to-noise ratios together with immunity from noise interference and makes possible high quality transmission at lower transmitter powers. The calculation carried out here for phase-shift-keying on a line

TABLE 5. BANDWIDTH REQUIREMENT FOR TRAIN COMMUNICATION WITH PCM-PSK.

Function	PCM Mode	No. of ckts.	Bw/ckt	Total BW
Command & Control	2 phase PSK	180	0.125 MHz	22.5 MHz
Passenger Telephone	4 phase PSK	360	0.0625 MHz	22.5 MHz
Operator Telephone	4 phase PSK	360	0.0625 MHz	22.5 MHz
News/PA	4 phase PSK	180	0.0625 MHz	11.25 MHz
Total (voice)		1080		78.75 MHz
Television	4 phase PSK	1		83 MHz
Overall total (TV & voice)				162 MHz

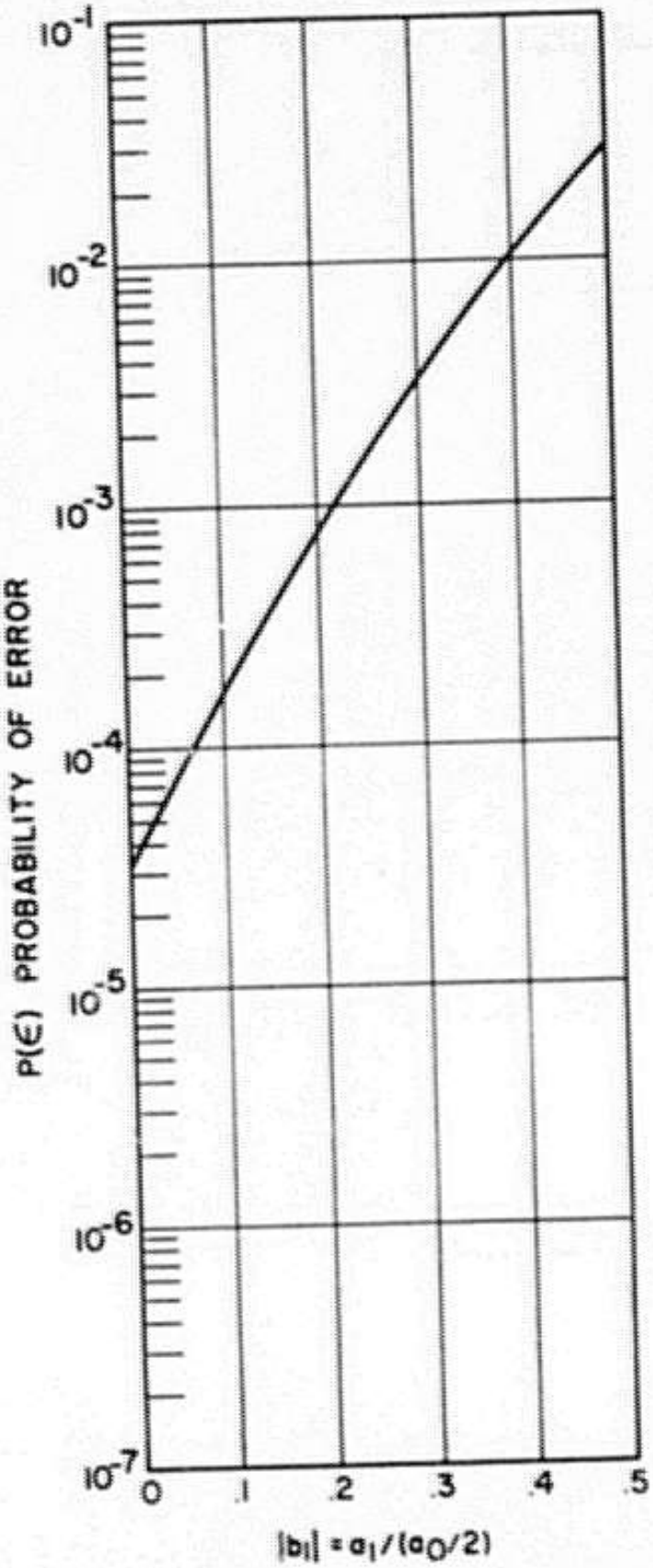

$|b_1|$ IS MAGNITUDE OF PHASE RIPPLE AMPLITUDE RADIANS

a_1 IS AMPLITUDE RIPPLE

$a_0/2$ IS ATTENUATION OF TRANSMISSION LINE

IT IS ASSUMED THAT BOTH b_1 AND a_1 ARE PRESENT AND THAT $|b_1| = a_1/(a_0/2)$

Figure 30. Probability of Error vs. Ripple Amplitude - Assuming $E/N_o = 8$ for no Ripple. Coherent PSK.

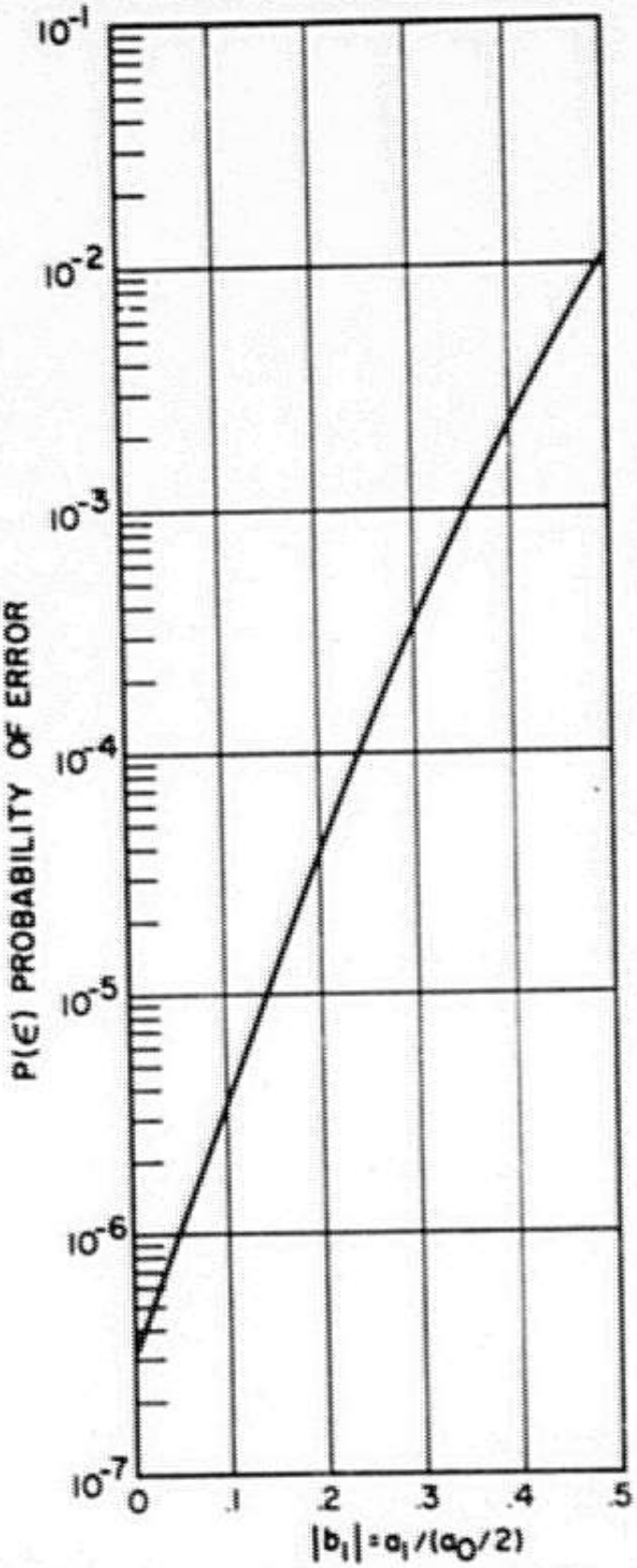

Figure 31. Probability of Error vs. Ripple Amplitude - Assuming E/N_o = 12.5 for no Ripple. Coherent PSK.

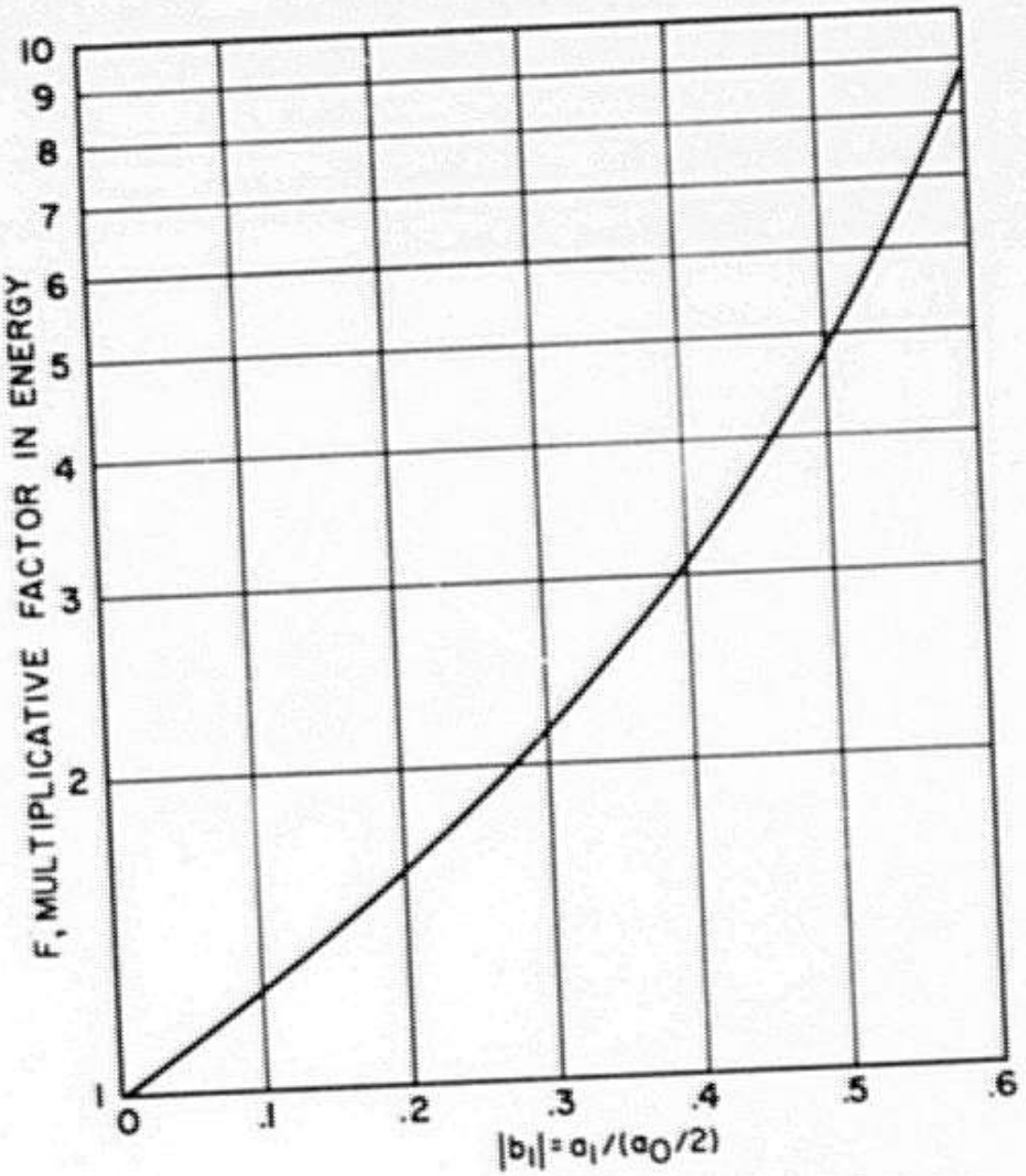

Figure 32. Multiplicative Factor in Energy Required to Offset Ripple Effect vs. Ripple Amplitude

with reflection discontinuities has shown that a fixed error criterion can be maintained at the expense of increased power. It remains to be seen, however, whether biphase PSK which is optimum in the presence of white Gaussian noise remains so when in the presence of interfering echoes. An alternative scheme might be FSK whose signal vectors are orthogonal in the sense that they do not interfere with each other. Thus, only echoes at the frequency of the bit being demodulated would contribute to the echo distortion.

It should therefore be emphasized that the choice of modulation should not be considered settled, and that the areas of signal design and channel equalization require further study before a final choice can be made.

BIBLIOGRAPHY

1. Panter, P.F.: Modulation, Noise and Spectral Analysis. McGraw-Hill, New York, 1965.

2. Lathi, B.P.: Communication Systems. John Wiley and Sons, Inc., New York, 1968.

3. Oliver, B.M., Pierce and Shannon, C.E.: The Philosophy of PCM, Proceedings of IRE, Nov. 1948, pp. 1324-1331.

4. Cattermole, K.W.: Principles of Pulse Code Modulation, American Elsevier Publishing Co., New York, 1969.

5. Reeves, A.H.: The Past, Present and Future of PCM, IEEE Spectrum, pp. 58-63, May, 1965.

6. Goodall, W.M.: Telephony by Pulse Code Modulation. Bell Systems Tech. J. Vol. 2b, July, 1947, No.3, pp. 395-409.

7. Meacham, L.A., Peterson, D.: An Experimental Multichannel Pulse Code Modulation System of Toll Quality. Bell System Tech. J. Vol. 27, January, 1948, No.1, pp. 1-43.

8. Akima, H.: The Error Rates in Multiple FSK Systems, Natl. Bur. of Standards Tech. Note 167, March, 1963.

9. Baghdady, E.J. and Tiller, J.L.: A Handbook of Digital Modulation and Demodulation Techniques Applicable to the Evaluation of the Saturn V Systems. Report NASA-CR-61407. ADCOM Inc., Cambridge, Ma., Contract NAS8-21078, Jan., 1968.

10. Lawton, J.G.: Comparison of Binary Data Transmission Systems, Proc. 2d Natl. Conf. Military Electronics, 1958, pp. 54-61.

11. Cahn, C.R.: Combined Digital Phase and Amplitude Modulation Communication Systems, IRE Trans. Communication Systems, Vol. CS-8, No. 3, pp. 150-155.

12. Wright, N.L., and Jolliffe, S.A.: Optimum System Engineering for Satellite Communication Links with Special Reference to the Choice of Modulation Method, J. Brit. IRE, May, 1962.

13. Hancock, J.C.: On Comparing the Modulation Systems, Proc. Natl. Electron, Conf., 1962, p. 49.

14. Physical Science Laboratory, New Mexico State University, Las Cruces, New Mexico, 88W01: Evaluation of FSM-FM Modulation for Use on Wayside Communication Systems, Final Report Contract No. DOT-FR-9-0026 with the Office of High Speed Ground Transportation, March 1970, PE00651 Report No. FRA-RT-70-37.

15. Goldman, S.: Frequency Analysis, Modulation and Noise, Dover Publications, Inc., New York, 1967, pp. 120-108.

16. Wheeler, H.A.: The Interpretation of Amplitude and Phase Distortion in Terms of Paired Echoes, Proc. IRE, June, 1939, p. 359.

17. Requirement and Methodology for Evaluation of the Wayside Communication Link, Physical Science Laboratory, New Mexico State University, Sept., 1969.

18. Tillotson, L.C.: Millimeter-Wavelength Radio Systems, Science, Vol. 170, Oct., 1970, pp. 31-36.

19. Tillotson, L.C.: Bell System Tech. J. 47, 2111, 1968.

20. Kirk, D. and Paolini, M.J.: A Digital Video System for the CATV Industry, Proc. IEEE, Vol. 58, No. 7, July, 1970, pp. 1026-1035.

21. Yoshida, K., Tachikawa, K., Tanaka, R. and Fukeda, H.: 2 GHz Microwave PCM System, Japan Telecommunication Review 11, pp. 18-29 (1969).

22. Mayo, J.S.: Experimental 224 mb/s PCM Terminals. Bell System Tech. J. 44, pp. 1813-41, Nov., 1965.